
Vision-driven Preference Synthesis for Mitigating Hallucinations in VLMs

Yunhun Nam Jongheon Jeong
Korea University
{yh0326, jonghj}@korea.ac.kr

Abstract

Vision-Language Models (VLMs) have shown strong performance in visual understanding, yet they still suffer from hallucinations, generating content that is not grounded in the image. Preference alignment is a promising approach to improve visual faithfulness, but its success depends heavily on how preference pairs are constructed. Existing methods exhibit two key limitations; (a) intervention-based methods often introduce significant deviation from the policy distribution, and (b) sampling-based methods often underuse visual information during the construction. In this paper, we propose ViPSy (**V**ision-driven **P**reference **S**ynthesis), a framework for constructing preference data that are both policy-aligned and visually grounded. Our framework consists of two stages; in the first stage, ViPSy derives a visual cue from recurring object-level content across semantically aligned image variants, so preference construction can rely on visual information rather than language priors. In the second stage, ViPSy conditions the policy’s own rollouts on this cue, allowing candidates to be guided by visually grounded content while staying close to the policy’s response distribution. The resulting candidates remain close to the policy’s response distribution while better leveraging visual information from the image. Experiments show that the resulting VLM, preference-aligned with ViPSy-constructed preference pairs, achieves a new state-of-the-art in hallucination mitigation. Compared with the previous state-of-the-art method, it reduces hallucination rates on AMBER and Object HalBench by 35.7% and 24.5%, respectively. The resulting model further improves on general visual grounding benchmarks, e.g., MMStar, MMVP, and CV-Bench, while also yielding gains in semantic segmentation and ImageNet linear probing, underscoring the effectiveness of our framework in enhancing the model’s visual capabilities. Code is available at <https://github.com/yunpal/ViPSy>.

1 Introduction

Recent progress in Vision-Language Models (VLMs) [1–5] has led to notable improvements in visual understanding. By combining pretrained vision encoders [6, 7] with Large Language Models (LLMs) [8, 9], VLMs can jointly process images and text, supporting vision-language applications across diverse domains, including education [10, 11], medical applications [12–14], industrial inspection [15–17], and robotics [18–20]. Despite these capabilities, VLMs still suffer from a fundamental limitation known as *hallucination* [21, 22], *i.e.*, generating content inconsistent with the given image, often introducing objects that do not actually exist. This limitation raises concerns about the reliability of VLMs in real-world applications, making hallucinations a critical challenge to address.

Hallucination in VLMs often arises from imbalances between the language and vision modalities, where strong language priors make models rely on text instead of the image [23–27]. Hallucination is also associated with statistical biases in pre-trained data [28–31], which can cause models to favor frequent but visually unsupported associations. To address these issues, preference-based alignment

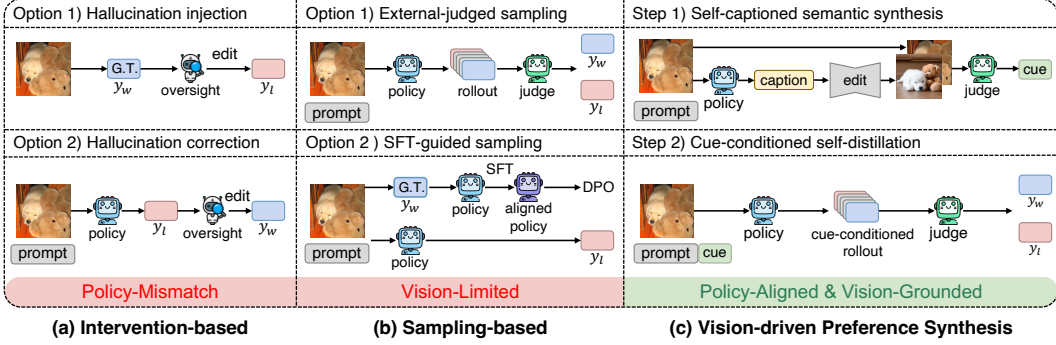


Figure 1: Comparison of preference construction strategies for hallucination mitigation in VLMs. (a) Intervention-based methods can create preference pairs that deviate from the policy distribution. (b) Sampling-based methods reduce this mismatch, but underuse visual information. (c) ViPSy addresses both issues through self-captioned semantic synthesis for consistent cue extraction and cue-conditioned self-distillation for preference synthesis.

[32–34] has emerged as a promising direction for improving the visual faithfulness of VLMs. In particular, hallucination mitigation can be naturally formulated as a preference optimization, where hallucination-free responses are treated as preferred outputs over hallucinated ones under the same image and prompt. For hallucination mitigation in VLMs, Direct Preference Optimization (DPO) [35] has become a practical choice for preference alignment, as it directly optimizes the model from preference pairs without explicit reward modeling or online rollouts. By avoiding these requirements, DPO sidesteps the challenges of reinforcement learning (RL), which updates a policy to maximize preference-derived rewards [36–39]. Specifically, reliable image-grounded rewards are difficult to define due to vision-language misalignment [40], and RL-based methods further require reward modeling and repeated online rollouts [35, 41–43].

Nevertheless, the effectiveness of DPO largely depends on the quality of the constructed preference pairs [44, 45]. As shown in Figure 1, existing methods for hallucination mitigation differ mainly in how they construct such pairs and can be grouped into (a) intervention-based and (b) sampling-based methods. Intervention-based methods include hallucination injection methods [46, 47], which create rejected responses by inserting hallucinated content into correct responses, and hallucination correction methods [40, 32, 48], which revise model-generated responses. Although these methods can provide explicit hallucinated and hallucination-free pairs, their responses are partially determined by external intervention and thus deviate from the policy distribution. Sampling-based methods rather aim to reduce this distribution mismatch by making preference data closer to the policy [49, 34, 33]. External-judged sampling methods construct preference pairs from the policy’s rollouts and use a judge to determine preferred and dispreferred responses [49, 33]. Supervised fine-tuning (SFT)-guided sampling first performs SFT on hallucination-free responses and then aligns the resulting model with pairs that favor SFT-aligned outputs over pre-SFT outputs [34]. Although policy-aligned preference data can improve the effectiveness of preference optimization [50–52], existing methods still lack the use of visual information.

Contributions. In this paper, we propose ViPSy (**V**ision-driven **P**reference **S**ynthesis), a framework for hallucination mitigation that constructs visually grounded preference pairs while keeping them close to the policy’s response distribution. The framework addresses two challenges in preference construction: limited use of visual information and distribution mismatch with the policy. First, we introduce *self-captioned semantic synthesis* for consistent cue extraction. Using the policy’s own self-captions as T2I prompts, we synthesize semantically aligned image variants. Comparing these variants with the original image reveals recurring object-level evidence, which is aggregated into a consistent visual cue. This cue provides explicit visual guidance for preference construction, reducing reliance on language priors. Second, we introduce *cue-conditioned self-distillation* for preference synthesis. The consistent visual cue guides the policy’s own rollouts, producing cue-conditioned self-generated candidate responses. We then select visually grounded and less grounded responses from these candidates. Thus, the cue encourages visual grounding, while the policy’s own rollouts keep the resulting pairs close to its distribution.

Experimental results show that ViPSy enables a new state-of-the-art in mitigating hallucinations of VLMs when used for DPO. Compared to the previous state-of-the-art results, our method significantly reduces AMBER CHAIR and Object HalBench response-level hallucination by 35.7% and 24.5%, respectively. Interestingly, we observe that our alignment scheme further improves general vision-language benchmarks that require visual grounding, with gains of 6.0% on MMStar, 31.3% on MMVP, and 4.0% on CV-Bench. Moreover, the optimized vision encoder shows gains in patch-level segmentation probing and ImageNet linear probing, suggesting improvements in both response-level visual faithfulness and visual representations.

We summarize the key contributions of this work as follows:

- We propose ViPSy, a vision-driven preference synthesis framework that constructs visually grounded preference pairs while keeping them close to the policy’s response distribution.
- We introduce a two-stage preference construction strategy: self-captioned semantic synthesis for extracting a consistent visual cue, and cue-conditioned self-distillation for generating policy-aligned candidate responses guided by the cue.
- We show that ViPSy sets a new state-of-the-art in hallucination mitigation, improves general vision-language benchmarks requiring visual grounding, and further enhances the visual representations of the underlying vision encoder.

2 Related work

Preference alignment. Preference alignment aims to make model outputs better reflect human preferences. A representative approach is Reinforcement Learning from Human Feedback (RLHF) [38, 40], which trains a reward model to judge rollout preferences and then optimizes the policy with PPO [53]. This framework has been used for aligning models to be helpful [39], while AI feedback can reduce reliance on human preference labeling [54, 48, 49]. Recent RL variants such as Group Relative Policy Optimization (GRPO) reduce policy-optimization cost with group-relative rewards [55], but still require rollout-level reward evaluation, which is difficult to define for VLM hallucination mitigation under vision-language misalignment [40]. DPO [35] instead learns from pre-constructed preferred and dispreferred response pairs, avoiding explicit reward modeling or online RL and shifting the key challenge to preference construction. Building on the same preference optimization perspective, related methods have explored alternative objectives, including sequence-level likelihood calibration [56], general theoretical objectives for learning from preferences [57], alignment from binary desirable or undesirable feedback [58], and optimization without a reference model [59, 60]. Preference-based methods further improve visual faithfulness by modifying alignment objectives [61–64]. These works provide diverse preference optimization objectives, while our work complements them by constructing visually grounded preference data for VLM hallucination mitigation.

Mitigating hallucination in VLMs. Motivated by this shift from reward design to preference-data construction, hallucination mitigation in VLMs focuses on constructing visually grounded preference pairs, where preferred responses should be faithful to the image while dispreferred responses capture hallucinated or unsupported content. Preference-construction methods differ in how response pairs are obtained. Intervention-based methods construct pairs by modifying responses or visual inputs, including hallucination injection [46], hallucination correction [32], segment-level correction [65], semantic-component manipulation [66], phrase modification in ground-truth descriptions [47], and distorted images [67]. In contrast, sampling-based methods derive pairs from policy-generated responses using external judges [49], SFT-guided on-policy alignment [34], detector-based verification [33], which relies on detector models [68, 69]. Our work follows this sampling-based direction while further incorporating visual information through visual cues extracted from self-captioned semantic synthesis and cue-conditioned self-distillation for preference synthesis.

Policy-aligned self-generated data. Sampling-based methods build on the observation that learning can benefit from training data that is close to the policy distribution [70, 50]. This perspective has motivated a broad range of self-generation approaches, including self-generated instructions [71], self-generated rewards [72], self-play preferences [73], synthetic preference data [74], and policy-aligned self-distillation [51, 52]. However, these methods do not explicitly account for visual inputs during self-generation. When an image is provided, the resulting supervision can therefore be driven by language priors rather than the visual information in the image. ViPSy addresses this

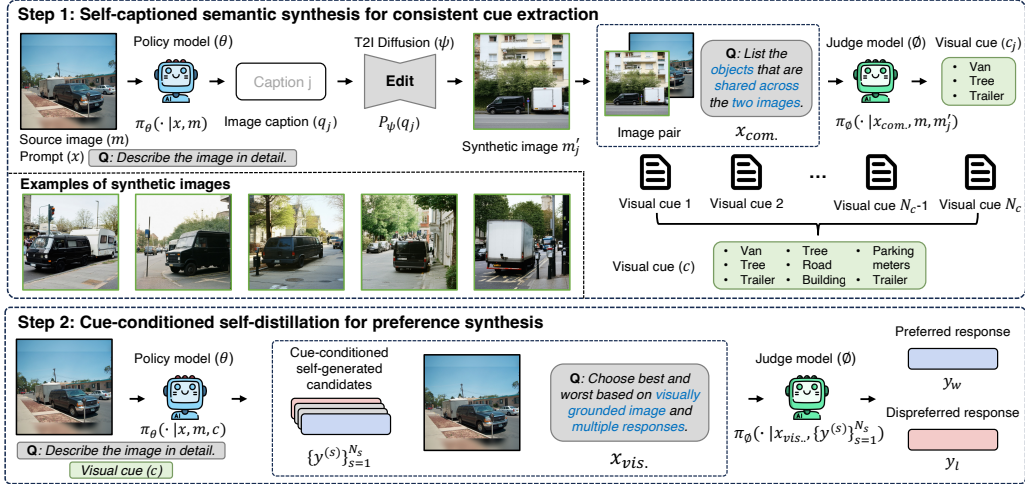


Figure 2: **Overview of ViPSy.** ViPSy constructs visually grounded and policy-aligned preference pairs through two stages. (1) *Self-captioned semantic synthesis for consistent cue extraction* uses the policy’s own self-captions as T2I prompts to generate semantically aligned synthetic variants. Each variant is compared with the original image, and recurring object-level evidence across comparisons is aggregated into a consistent visual cue. (2) *Cue-conditioned self-distillation for preference synthesis* uses the consistent visual cue to guide the policy’s own rollouts, producing cue-conditioned self-generated candidate responses. A judge model then selects preferred and dispreferred responses according to their visual grounding with respect to the original image.

limitation by conditioning the policy’s own rollouts on consistent visual cues, keeping the generated data close to the policy distribution while making its construction explicitly vision-grounded.

3 ViPSy: Vision-driven Preference Synthesis

We consider a vision-language model that generates a response \mathbf{y} conditioned on a prompt \mathbf{x} and an input image \mathbf{m} , given a policy π_θ parameterized by θ :

$$\pi_\theta(\mathbf{y} \mid \mathbf{x}, \mathbf{m}) = \prod_{t=1}^T \pi_\theta(\mathbf{y}_t \mid \mathbf{x}, \mathbf{m}, \mathbf{y}_{<t}). \quad (1)$$

Preference construction for hallucination mitigation requires pairs that contrast visually faithful responses with image-unsupported ones. Intervention-based methods create such contrasts by externally modifying responses, but this can move the data away from the policy distribution. Sampling from the policy reduces this mismatch; however, even when the policy is conditioned on the image \mathbf{m} in Eq. 1, its rollouts may still be driven by language priors or modality biases rather than image-specific evidence. We therefore aim to construct preference pairs that remain close to the policy distribution while using object-level visual cues extracted from the image as additional conditioning for the policy’s own rollouts.

As summarized in Figure 2, ViPSy achieves this goal by extracting a consistent visual cue from semantically aligned image variations, as detailed in Section 3.1. The key intuition is that visual content present in the original image should recur across synthetic images generated from diverse captions describing the same image. This consistent visual cue is then used to guide cue-conditioned self-rollouts from the policy, as described in Section 3.2. Rather than constructing preferences from externally generated responses, we sample cue-conditioned self-generated candidate responses from the policy itself. Thus, the visual cue encourages visual grounding, while the policy’s own rollouts keep the candidates close to its response distribution.

3.1 Self-captioned semantic synthesis for visual cue extraction

To construct semantically aligned synthetic images, we use the policy’s captions of images as T2I prompts. Concretely, we define the captioning prompt as $\mathbf{x}_{\text{cap.}} = \text{“Describe the image in detail.”}$. We sample N_c captions and synthesize their corresponding images using a T2I diffusion model P_ψ :

$$\{\mathbf{q}_j\}_{j=1}^{N_c} \sim \pi_\theta(\cdot \mid \mathbf{x}_{\text{cap.}}, \mathbf{m}), \quad \{\mathbf{m}'_j\}_{j=1}^{N_c} = \{P_\psi(\mathbf{q}_j)\}_{j=1}^{N_c}. \quad (2)$$

Although the sampled captions are grounded in the same image, they emphasize different aspects of the image. Since these images share the same underlying semantic content, comparing them against the original image helps identify image-supported evidence.

Visual cue extraction. From the self-captioned synthetic images \mathbf{m}'_j , we extract a pairwise cue \mathbf{c}_j for each \mathbf{m}'_j by comparing it with the original image. Specifically, for the synthetic image indexed by j , the judge model extracts object-level visual evidence that is consistent between the original image \mathbf{m} and the corresponding synthetic image \mathbf{m}'_j :

$$\mathbf{c}_j = \pi_\phi(\mathbf{x}_{\text{comp.}}, \mathbf{m}, \mathbf{m}'_j), \quad (3)$$

where ϕ denotes a judge model and $\mathbf{x}_{\text{comp.}}$ is the pairwise comparison prompt provided in Appendix I. The pairwise cues are then aggregated into a consistent visual cue:

$$\mathbf{c} = \pi_\phi(\mathbf{x}_{\text{agg.}}, \{\mathbf{c}_j\}_{j=1}^{N_c}), \quad (4)$$

where $\mathbf{x}_{\text{agg.}}$ is the aggregation prompt provided in Appendix I. Since T2I introduces variations in visual appearance, cues that recur consistently across multiple pairwise comparisons are more likely to reflect content grounded in the original image. The aggregation combines these pairwise consistent cues to produce the consistent visual cue \mathbf{c} , which serves as guidance for preference construction.

3.2 Cue-conditioned self-distillation for preference synthesis

The visual cue \mathbf{c} guides the policy’s own rollouts. We sample N_s cue-conditioned self-generated candidate responses from the policy:

$$\mathbf{y}^{(s)} \sim \pi_\theta(\cdot \mid \mathbf{x}_{\text{cue-cap.}}, \mathbf{m}, \mathbf{c}), \quad (5)$$

where s indexes the sampled candidate responses and $\mathbf{x}_{\text{cue-cap.}}$ denotes the cue-conditioned captioning prompt provided in Appendix I. Repeated sampling under the same prompt, image, and visual cue produces diverse cue-conditioned candidate responses. Since these candidates are sampled from the policy itself, they remain close to the policy’s response distribution, while the visual cue encourages them to leverage visual information from the image, resulting in varying degrees of visual grounding across candidates.

Preference selection by visual grounding. From the cue-conditioned candidate responses $\{\mathbf{y}^{(s)}\}_{s=1}^{N_s}$, we select a preferred response \mathbf{y}_w and a dispreferred response \mathbf{y}_l based on visual grounding. Specifically, we query the judge model with a visual grounding prompt:

$$(\mathbf{y}_w, \mathbf{y}_l) = \pi_\phi(\mathbf{x}_{\text{vis.}}, \mathbf{m}, \{\mathbf{y}^{(s)}\}_{s=1}^{N_s}), \quad (6)$$

where $\mathbf{x}_{\text{vis.}}$ is the visual grounding prompt provided in Appendix I. The prompt asks the judge model to compare the candidate responses with respect to the original image \mathbf{m} . The selected pair contrasts a more visually grounded response with a less grounded one, forming a policy-aligned preference pair from the policy’s own cue-conditioned generations. We provide the ViPSy algorithm in Appendix F.

3.3 Preference optimization with ViPSy

Once ViPSy constructs the preference dataset $\mathcal{D}_{\text{pref}} = (\mathbf{x}_i, \mathbf{m}_i, \mathbf{y}_{w,i}, \mathbf{y}_{l,i})$, the pairs can be used with a range of pairwise preference optimization objectives [56, 57, 59, 60]. We instantiate this step with DPO [35] to match the optimization objective used in recent hallucination mitigation methods, enabling a fair comparison while isolating the effect of our preference construction. We optimize:

$$\mathcal{L}_{\text{DPO}} = -\mathbb{E}_{(\mathbf{x}, \mathbf{m}, \mathbf{y}_w, \mathbf{y}_l) \sim \mathcal{D}_{\text{pref}}} \left[\log \sigma \left(\beta \log \frac{\pi_\theta(\mathbf{y}_w \mid \mathbf{x}, \mathbf{m})}{\pi_{\text{ref}}(\mathbf{y}_w \mid \mathbf{x}, \mathbf{m})} - \beta \log \frac{\pi_\theta(\mathbf{y}_l \mid \mathbf{x}, \mathbf{m})}{\pi_{\text{ref}}(\mathbf{y}_l \mid \mathbf{x}, \mathbf{m})} \right) \right], \quad (7)$$

Table 1: Comparison on hallucination and general benchmarks using LLaVA-1.5-7B & LLaVA-1.5-13B [1]. **Bold** and underline values indicate the best and second-best results, respectively.

Model	Method	Hallucination benchmarks						General benchmarks		
		Object HalBench		AMBER			HallusionBench	MMStar	MMVP	CV-Bench
		Resp.↓	Ment.↓	CHAIR↓	Hal.↓	Cog.↓	aAcc.↑	Acc.↑	Acc.↑	Acc.↑
LLaVA-1.5-7B	Vanilla	51.3	25.9	7.9	36.8	4.3	46.8	33.4	23.3	61.9
	VCD [27]	50.6	25.6	8.1	37.9	4.0	47.2	<u>34.5</u>	25.3	56.0
	DOLA [75]	44.3	24.9	6.5	28.5	3.1	46.7	33.5	22.6	62.0
	OPERA [76]	42.0	22.6	5.8	27.7	3.0	45.7	33.4	22.6	61.9
	EFUF [77]	41.6	22.6	5.8	28.2	3.0	47.0	33.6	24.6	62.2
	LLaVA-RLHF [40]	52.6	26.9	9.8	46.4	5.4	41.8	20.1	12.0	27.8
	HALVA [47]	41.3	20.5	6.8	33.3	3.5	48.8	32.7	23.3	61.3
	HA-DPO [32]	39.0	19.6	6.6	30.9	3.2	<u>48.1</u>	32.7	22.6	61.4
	POVID [46]	31.6	16.3	5.4	28.7	3.0	46.5	33.6	25.3	62.6
	TPR [66]	11.0	5.8	3.6	20.4	1.7	39.8	33.2	<u>29.3</u>	<u>63.6</u>
	RLAIF-V [49]	8.6	4.1	2.9	15.8	<u>0.9</u>	35.1	34.0	24.0	42.4
	OPA-DPO [34]	8.6	5.1	<u>2.7</u>	13.7	1.1	47.9	32.8	28.0	59.5
	SENTINEL [33]	<u>5.3</u>	<u>3.0</u>	2.8	<u>13.6</u>	1.2	47.6	33.6	24.6	61.9
ViPSy (Ours)		4.0	2.6	1.8	9.6	0.6	<u>48.1</u>	35.4	30.6	64.4
LLaVA-1.5-13B	Vanilla	44.6	22.1	5.9	28.1	4.1	46.5	33.2	32.0	61.7
	HALVA [47]	47.3	12.8	5.8	28.8	4.1	<u>47.6</u>	33.4	32.6	<u>61.4</u>
	LLaVA-RLHF [40]	36.3	11.8	6.8	34.1	5.2	45.9	20.5	21.3	37.6
	HSA-DPO [48]	5.0	3.0	2.2	12.2	1.6	46.1	34.5	<u>33.3</u>	60.1
	OPA-DPO [34]	6.0	3.7	<u>2.1</u>	<u>9.4</u>	1.4	46.4	<u>34.6</u>	31.3	61.3
	SENTINEL [33]	<u>3.3</u>	<u>1.9</u>	2.4	11.9	<u>1.2</u>	47.4	32.4	35.3	60.5
ViPSy (Ours)		2.6	1.3	1.9	9.2	1.1	48.0	35.8	35.3	62.6

where π_{ref} denotes the reference policy and β is a scaling parameter. The consistent visual cue c and self-captioned synthetic images $\{m_j\}_{j=1}^K$ are used only for constructing the preference pairs, not as inputs to the policy or reference model during DPO. During optimization, the policy and reference model evaluate the constructed responses (y_w, y_l) conditioned only on the original prompt-image pair (x, m) . This design enables cue-conditioned self-distillation by using preference optimization to distill cue-guided visual grounding into the image-conditioned policy. Consequently, ViPSy improves visual grounding without requiring cue extraction or synthetic image generation at inference time.

4 Experiments

Our experiments evaluate whether ViPSy addresses the two limitations identified above: (a) policy-distribution mismatch in intervention-based methods and (b) limited use of visual information in sampling-based preference construction. To validate it, we assess whether the constructed preference pairs reduce hallucination while enhancing general vision-language capability, and further examine whether self-derived visual cues strengthen the vision encoder through visual representation and segmentation evaluations rather than merely suppressing language-prior-driven hallucination.

4.1 Setups

Models. Following prior work, we use LLaVA-1.5-7B and LLaVA-1.5-13B [1] as the policy models for direct comparison with existing hallucination mitigation methods. We use Qwen2.5-VL-72B [78] as the default judge model and SD-3.5-L [79] as the default T2I diffusion model for semantic synthesis. To test whether the proposed preference construction is policy-agnostic, we further evaluate diverse VLMS, including Qwen2.5-VL-7B [78], InternVL3.5-8B [80], mPLUG-Owl3-7B [81], and Kimi-VL-A3B [82]. We also consider Qwen3-VL-30B [4] and GPT-5 mini [83] as alternative judges, and SD-3.5-M [79], Flux-1.0-dev [84], and PixelDiT [85] as alternative T2I models in ablations. Additional details on policy, judge, and diffusion models are provided in Appendix C.

Baselines. We compare ViPSy with hallucination-mitigation baselines, including decoding methods [27, 75, 76], which work only at inference time, and unlearning-based methods [77], which use curated data. Intervention-based methods [32, 46, 47, 66, 48] can deviate from the policy distribution, while sampling-based methods [40, 49, 34, 33] often underuse visual information during preference construction. Detailed descriptions are provided in Appendix D.

Table 2: Average hallucination and general benchmark scores across policy models.

Method	Hal. Avg. ↓	Gen. Avg. ↑
Qwen2.5-VL-7B		
Vanilla	9.48	64.90
ViPSy	8.16	66.10
mPLUG-Owl3-7B		
Vanilla	6.66	48.87
ViPSy	5.84	50.10
InternVL3.5-8B		
Vanilla	8.66	69.07
ViPSy	6.78	69.77
Kimi-VL-A3B		
Vanilla	11.52	57.97
ViPSy	8.70	59.53

Table 3: Ablation study on model configurations based on average scores across hallucination [87, 88] and general benchmarks [89–91], respectively. “Self” denotes sampling from LLaVA-1.5-7B.

ViPSy Configuration			Benchmarks	
I→T	T→I	Rollout	Hal. Avg. ↓	Gen. Avg. ↑
<i>Vanilla (LLaVA-1.5-7B)</i>			25.24	39.53
Self	SD-3.5-L	Self	3.72	43.47
GPT-5 mini	SD-3.5-L	Self	5.12	42.57
Qwen3-VL-30B	SD-3.5-L	Self	4.70	42.13
Qwen2.5-VL-72B	SD-3.5-L	Self	4.26	42.40
Self	PixelDiT	Self	4.50	42.70
Self	Flux-1.0-dev	Self	4.36	42.50
Self	SD-3.5-M	Self	3.86	42.87
Self	SD-3.5-L	GPT-5 mini	15.64	41.07
Self	SD-3.5-L	Qwen3-VL-30B	16.00	42.07
Self	SD-3.5-L	Qwen2.5-VL-72B	11.22	41.80

Table 4: Vision encoder evaluation with 2-, 4-, and 8-shot linear probing accuracy on ImageNet-1k (IN-1k), ImageNet-O (IN-O), and Rendered-SST2 (R-SST2), and segmentation recall on MS COCO.

Method	Linear Probing									Seg.
	2-shot			4-shot			8-shot			MS COCO Recall ↑
	IN-1k Acc.↑	IN-O Acc.↑	R-SST2 Acc.↑	IN-1k Acc.↑	IN-O Acc.↑	R-SST2 Acc.↑	IN-1k Acc.↑	IN-O Acc.↑	R-SST2 Acc.↑	
Vanilla	35.4	18.0	48.9	48.6	29.5	50.4	59.3	38.0	50.1	34.7
ViPSy (Ours)	36.1	18.3	49.5	49.0	30.0	51.0	60.0	38.5	50.9	35.9

Datasets and evaluation. We construct preference data from Visual Genome images [86], following Peng et al. [33], with implementation and training details in Appendix B. We evaluate hallucination on Object HalBench [87], AMBER [88], and HallusionBench [22], and general vision-language capability on MMStar [89], MMVP [90], and CV-Bench [91]. For vision encoder evaluation, we use ImageNet 1k [92], ImageNet-O [93], and Rendered-SST2 [94, 6] for linear probing, and MS COCO [95] for segmentation. Dataset and metric details are provided in Appendix E.

4.2 Main results

Mitigating hallucination. Table 1 shows that ViPSy achieves state-of-the-art hallucination mitigation on LLaVA-1.5-7B and remains effective on LLaVA-1.5-13B. On LLaVA-1.5-7B, against TPR [66], the strongest intervention-based method, our method reduces Object HalBench Resp./Ment. by 63.6%/55.2% and AMBER CHAIR/Hal./Cog. by 50.0%/52.9%/64.7%. Against the strongest sampling-based, SENTINEL [33], it improves Object HalBench Resp./Ment. by 24.5%/13.3% and AMBER CHAIR/Hal./Cog. by 35.7%/29.4%/50.0%. These gains support policy-aligned, visually grounded preference construction. Although it ranks second on HallusionBench, it achieves the best results on the remaining benchmarks, showing broader gains in faithful visual understanding. On the larger LLaVA-1.5-13B model, ViPSy outperforms all baselines across all hallucination benchmarks. In particular, compared with the previous state-of-the-art, it achieves notable improvements of 21.2%/31.6% on Object HalBench Resp./Ment. and 20.8%/22.7%/8.3% on AMBER CHAIR/Hal./Cog. These results indicate that ViPSy remains effective as the model scales. Qualitative examples in Appendix H.2 show that preference-aligned descriptions using preference pairs constructed by our method avoid unsupported details and produce image-grounded descriptions.

General performance. On general benchmarks with LLaVA-1.5-7B, our preference construction improves over vanilla on all three benchmarks, with gains of 6.0% on MMStar, 31.3% on MMVP, and 4.0% on CV-Bench, achieving the best overall results among compared methods. Unlike sampling-based methods that degrade or merely maintain CV-Bench, our method improves it, suggesting that visual cues enhance general vision-language capability. Together with the hallucination results, these gains support policy-aligned, visually grounded preference pairs. The results on LLaVA-1.5-13B further demonstrate scalability, as our method outperforms all compared methods across all benchmarks and, in particular, improves over vanilla by 7.8% on MMStar and 10.3% on MMVP.

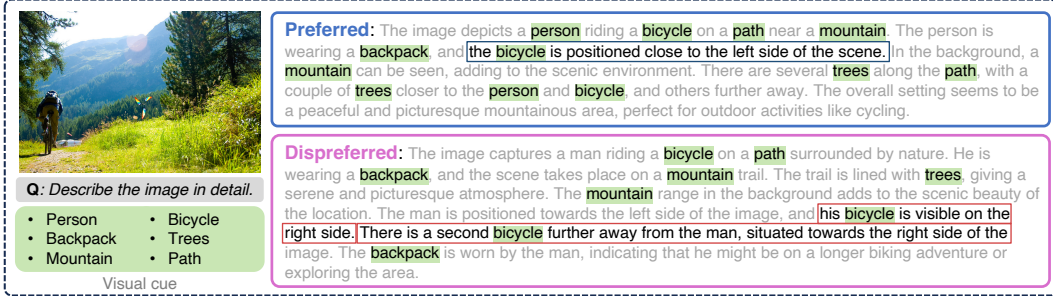


Figure 3: Qualitative examples of cue-conditioned preference pairs. Given the same image, prompt, and visual cue, preferred responses remain image-grounded, while dispreferred ones hallucinate. Additional examples are shown in Appendix H.1, H.2, and H.3: preference pairs, aligned-policy image descriptions, and self-captioned semantic synthesis, respectively.

Generalization across policy models. The effectiveness of ViPSy is not specific to LLaVA-1.5-7B. Table 2 shows that our method consistently generalizes across diverse policy models, improving both hallucination mitigation and general vision-language capabilities. Compared with the vanilla policy, it reduces the hallucination average, computed over two hallucination benchmarks [87, 88], by 13.9% on Qwen2.5-VL-7B, 12.3% on mPLUG-OwI3-7B, 21.7% on InternVL3.5-8B, and 24.5% on Kimi-VL-A3B. At the same time, it improves the general average across three general benchmarks [89–91]. These results demonstrate that policy-aligned, visually grounded preference construction provides consistent benefits beyond a single policy model. Full results are provided in Appendix G.1.

4.3 Analysis

Effect on vision encoder. To examine whether our approach improves the vision encoder beyond response-level hallucination mitigation, we use few-shot linear probing and segmentation. We update the vision encoder during preference alignment and freeze the resulting encoder for linear probing and segmentation. Following Liu et al. [96], we freeze the resulting vision encoder and train dataset-specific linear classifiers on frozen image features under 2-, 4-, and 8-shot settings. For segmentation, we train a two-layer transformer output head to predict patch-level semantic labels, following Covert et al. [97]. As shown in Table 4, our method improves ImageNet-1k, ImageNet-O, and Rendered-SST2 accuracy as well as segmentation recall over vanilla. These gains suggest that ViPSy improves both visual representation quality and the ability to separate visual regions, rather than merely suppressing language-prior-driven hallucinations in responses.

Qualitative analysis of cue-conditioned rollouts. We show how ViPSy obtains preferred and dispreferred responses, and we present examples of preference pairs selected from multiple cue-conditioned rollouts under the same image, prompt, and visual cue. Preferred responses use the visual cue to ground the image description, whereas dispreferred responses use the cue but add details unsupported by the image. As highlighted in Figure 3, the same visual cue can yield candidates with different grounding quality, e.g., in the bicycle scene, the preferred response correctly locates the bicycle close to the left side of the scene, while the dispreferred response states that the bicycle is on the right side and further hallucinates a second bicycle, although only one bicycle is visible. This demonstrates that preference selection is needed to separate faithful cue usage from unsupported extrapolation. More examples are provided in Appendix H.1.

Judge agreement and robustness. Since preference selection is performed by a judge over multiple cue-conditioned rollouts, one concern is whether the selected pairs depend on the judge model. We therefore evaluate the agreement between the default judge, Qwen2.5-VL-72B, and alternative judges. We also measure hallucination and general capabilities when each judge is used to construct preference pairs. As shown in Figure 4, Qwen3-VL-30B and GPT-5 mini agree with the default judge on 98.4% and 95.8% of preference selections, respectively, indicating that the selected preferences are highly consistent across judges. Furthermore, Table 9 shows that using different judges to construct preference pairs leads to similar results on both hallucination and general benchmarks. This suggests that the preference construction process is not dominated by judge-specific bias and that ViPSy reliably constructs visually grounded preference pairs. Detailed results are provided in Appendix G.4.

		y_l	y_w
GPT-5 mini	y_l	95.8%	4.2%
	y_w	4.2%	95.8%
Qwen3-VL-30B	y_l	98.4%	1.6%
	y_w	1.6%	98.4%
		y_l	y_w

Qwen2.5-VL-72B

Figure 4: Agreement of preference selections for alternative judges compared upon preferences based on Qwen2.5-VL-72B.

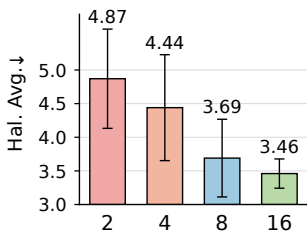


Figure 5: Effect of varying the number of cue-conditioned rollouts on average hallucination errors across five runs.

Strategy	Hal. Avg. ↓	Gen. Avg. ↑
Vanilla	25.24	39.53
w/o cue	7.14	42.50
Translation	5.10	43.13
Resize	4.82	42.47
Mask	4.82	42.53
Crop	4.76	42.43
Video	4.46	41.70
Diffusion	3.72	43.47

Table 5: Comparison of visual variations for cue extraction in average hallucination and general benchmark scores.

4.4 Ablation study

Visual cue construction. We analyze visual-cue construction by varying the captioning and T2I models. The input image is captioned, and the caption is used to synthesize an image for cue extraction. As shown in Table 3, self-captioning achieves the best overall result, while alternative T2I models remain competitive with moderate performance differences. This suggests that using policy-generated captions is beneficial for cue construction, and that ViPSy is not overly sensitive to the T2I model. Full results are in Appendix G.2, and Qualitative examples in Appendix H.3 show that self-captioned synthetic images preserve the main visual context while varying across T2I models.

Rollout model. We compare models for cue-conditioned rollout generation while keeping the visual-cue construction fixed. Self-rollouts achieve the best hallucination score and general performance, whereas rollouts from external VLMs lead to degraded results. This shows that candidate responses should remain close to the policy distribution while being guided by visual cues. Full results are provided in Appendix G.2.

Number of rollouts. To assess how the number of rollouts affects preference construction, we vary the number of cue-conditioned rollouts. As shown in Figure 5, more rollouts improve reliability by enlarging the candidate pool and increasing grounding-quality diversity. Increasing the number of rollouts reduces variance in hallucination score, as the larger candidate pool makes the preferred and dispreferred responses more clearly distinguishable. Since more rollouts can improve preference construction but increase computational cost, we use 8 cue-conditioned rollouts as a trade-off between reliability and efficiency. Additional results are included in Appendix G.3.

Cue conditioning and synthesis strategy. Table 5 studies cue conditioning and visual variation strategies for cue extraction. Even without cues, policy-sampled candidates improve over the vanilla model, but cue-conditioned construction performs better, confirming the importance of visual cues for visually faithful rollouts. Among cue extraction strategies, simple transformations such as translation, resize, mask, and crop bring improvements but provide limited semantic diversity. Video-based variation using an image-to-video model [98] can introduce uncontrolled changes. Diffusion-based synthesis produces richer semantic variations and achieves the best overall result, with the lowest hallucination score and the highest general capability. Detailed results are reported in Appendix G.5.

5 Conclusion

In this paper, we proposed ViPSy, a vision-driven preference synthesis that constructs preference pairs leveraging visual information while remaining aligned with the policy distribution. Unlike intervention-based methods that externally modify responses and sampling-based methods that overlook visual information, our approach first extracts visual cues by comparing the original image with semantically synthesized image variations. These cues then guide the policy model’s own rollouts, allowing candidate responses to remain close to the model’s generation distribution while encouraging them to leverage visual information from the input image. Experiments show that our approach achieves state-of-the-art hallucination mitigation while also improving general visual grounding benchmarks, with additional gains observed in vision encoder evaluations.

References

- [1] Haotian Liu, Chunyuan Li, Yuheng Li, and Yong Jae Lee. Improved Baselines with Visual Instruction Tuning. In *Proceedings of the IEEE/CVF conference on computer vision and pattern recognition*, pages 26296–26306, 2024.
- [2] Jean-Baptiste Alayrac, Jeff Donahue, Pauline Luc, Antoine Miech, Iain Barr, Yana Hasson, Karel Lenc, Arthur Mensch, Katherine Millican, Malcolm Reynolds, et al. Flamingo: a Visual Language Model for Few-Shot Learning. *Advances in neural information processing systems*, 35:23716–23736, 2022.
- [3] Wenliang Dai, Junnan Li, Dongxu Li, Anthony Tiong, Junqi Zhao, Weisheng Wang, Boyang Li, Pascale N Fung, and Steven Hoi. InstructBLIP: Towards General-purpose Vision-Language Models with Instruction Tuning. *Advances in neural information processing systems*, 36:49250–49267, 2023.
- [4] Shuai Bai, Yuxuan Cai, Ruizhe Chen, Keqin Chen, Xionghui Chen, Zesen Cheng, Lianghao Deng, Wei Ding, Chang Gao, Chunjiang Ge, et al. Qwen3-VL Technical Report. *arXiv preprint arXiv:2511.21631*, 2025.
- [5] OpenAI. GPT-4V(ision) System Card, 2023. URL <https://api.semanticscholar.org/CorpusID:263218031>.
- [6] Alec Radford, Jong Wook Kim, Chris Hallacy, Aditya Ramesh, Gabriel Goh, Sandhini Agarwal, Girish Sastry, Amanda Askell, Pamela Mishkin, Jack Clark, et al. Learning Transferable Visual Models From Natural Language Supervision. In *International conference on machine learning*, pages 8748–8763. PmLR, 2021.
- [7] Xiaohua Zhai, Basil Mustafa, Alexander Kolesnikov, and Lucas Beyer. Sigmoid Loss for Language Image Pre-Training. In *Proceedings of the IEEE/CVF international conference on computer vision*, pages 11975–11986, 2023.
- [8] Wei-Lin Chiang, Zhuohan Li, Zi Lin, Ying Sheng, Zhanghao Wu, Hao Zhang, Lianmin Zheng, Siyuan Zhuang, Yonghao Zhuang, Joseph E. Gonzalez, Ion Stoica, and Eric P. Xing. Vicuna: An Open-Source Chatbot Impressing GPT-4 with 90%* ChatGPT Quality, March 2023. URL <https://lmsys.org/blog/2023-03-30-vicuna/>.
- [9] Binyuan Hui, Jian Yang, Zeyu Cui, Jiayi Yang, Dayiheng Liu, Lei Zhang, Tianyu Liu, Jiajun Zhang, Bowen Yu, Keming Lu, et al. Qwen2.5-Coder technical report. *arXiv preprint arXiv:2409.12186*, 2024.
- [10] Pan Lu, Hritik Bansal, Tony Xia, Jiacheng Liu, Chunyuan Li, Hannaneh Hajishirzi, Hao Cheng, Kai-Wei Chang, Michel Galley, and Jianfeng Gao. MathVista: Evaluating Mathematical Reasoning of Foundation Models in Visual Contexts. *arXiv preprint arXiv:2310.02255*, 2023.
- [11] Unggi Lee, Minji Jeon, Yunseo Lee, Gyuri Byun, Yoorim Son, Jaeyoon Shin, Hongkyu Ko, and Hyeoncheol Kim. LLaVA-Docent: Instruction Tuning with Multimodal Large Language Model to Support Art Appreciation Education. *Computers and Education: Artificial Intelligence*, 7:100297, 2024.
- [12] Chunyuan Li, Cliff Wong, Sheng Zhang, Naoto Usuyama, Haotian Liu, Jianwei Yang, Tristan Naumann, Hoifung Poon, and Jianfeng Gao. LLaVA-Med: Training a Large Language-and-Vision Assistant for Biomedicine in One Day. *Advances in Neural Information Processing Systems*, 36:28541–28564, 2023.
- [13] Yizhen Luo, Jiahuan Zhang, Siqi Fan, Kai Yang, Yushuai Wu, Mu Qiao, and Zaiqing Nie. BioMedGPT: Open Multimodal Generative Pre-trained Transformer for BioMedicine. *arXiv preprint arXiv:2308.09442*, 2023.
- [14] Michael Moor, Qian Huang, Shirley Wu, Michihiro Yasunaga, Yash Dalmia, Jure Leskovec, Cyril Zakka, Eduardo Pontes Reis, and Pranav Rajpurkar. Med-Flamingo: a Multimodal Medical Few-shot Learner. In *Machine learning for health (ML4H)*, pages 353–367. PMLR, 2023.
- [15] Jongheon Jeong, Yang Zou, Taewan Kim, Dongqing Zhang, Avinash Ravichandran, and Onkar Dabeer. WinCLIP: Zero-/Few-Shot Anomaly Classification and Segmentation. In *Proceedings of the IEEE/CVF conference on computer vision and pattern recognition*, pages 19606–19616, 2023.
- [16] Zhaopeng Gu, Bingke Zhu, Guibo Zhu, Yingying Chen, Ming Tang, and Jinqiao Wang. AnomalyGPT: Detecting Industrial Anomalies Using Large Vision-Language Models. In *Proceedings of the AAAI conference on artificial intelligence*, volume 38, pages 1932–1940, 2024.
- [17] Xi Jiang, Jian Li, Hanqiu Deng, Yong Liu, Bin-Bin Gao, Yifeng Zhou, Jialin Li, Chengjie Wang, and Feng Zheng. MMAD: A Comprehensive Benchmark for Multimodal Large Language Models in Industrial Anomaly Detection. *arXiv preprint arXiv:2410.09453*, 2024.

- [18] Chuyan Xiong, Chengyu Shen, Xiaoqi Li, Kaichen Zhou, Jeremy Liu, Ruiping Wang, and Hao Dong. AIC MLLM: Autonomous Interactive Correction MLLM for Robust Robotic Manipulation. *arXiv preprint arXiv:2406.11548*, 2024.
- [19] Jinyi Liu, Yifu Yuan, Jianye Hao, Fei Ni, Lingzhi Fu, Yibin Chen, and Yan Zheng. Enhancing Robotic Manipulation with AI Feedback from Multimodal Large Language Models. *arXiv preprint arXiv:2402.14245*, 2024.
- [20] Xiaoqi Li, Mingxu Zhang, Yiran Geng, Haoran Geng, Yuxing Long, Yan Shen, Renrui Zhang, Jiaming Liu, and Hao Dong. ManipLLM: Embodied Multimodal Large Language Model for Object-Centric Robotic Manipulation. In *Proceedings of the IEEE/CVF Conference on Computer Vision and Pattern Recognition*, pages 18061–18070, 2024.
- [21] Anisha Gunjal, Jihan Yin, and Erhan Bas. Detecting and Preventing Hallucinations in Large Vision Language Models. In *Proceedings of the AAAI Conference on Artificial Intelligence*, volume 38, pages 18135–18143, 2024.
- [22] Tianrui Guan, Fuxiao Liu, Xiyang Wu, Ruiqi Xian, Zongxia Li, Xiaoyu Liu, Xijun Wang, Lichang Chen, Furong Huang, Yaser Yacoob, et al. HallusionBench: An Advanced Diagnostic Suite for Entangled Language Hallucination and Visual Illusion in Large Vision-Language Models. In *Proceedings of the IEEE/CVF conference on computer vision and pattern recognition*, pages 14375–14385, 2024.
- [23] Yike Wu, Yu Zhao, Shiwan Zhao, Ying Zhang, Xiaojie Yuan, Guoqing Zhao, and Ning Jiang. Overcoming Language Priors in Visual Question Answering via Distinguishing Superficially Similar Instances. In *Proceedings of the 29th International Conference on Computational Linguistics*, pages 5721–5729, 2022.
- [24] Yudong Han, Liqiang Nie, Jianhua Yin, Jianlong Wu, and Yan Yan. Visual Perturbation-aware Collaborative Learning for Overcoming the Language Prior Problem. *arXiv preprint arXiv:2207.11850*, 2022.
- [25] Ren Zhibo, Wang Huizhen, Zhu Muhua, Wang Yichao, Xiao Tong, and Zhu Jingbo. Overcoming Language Priors with Counterfactual Inference for Visual Question Answering. In *Proceedings of the 22nd Chinese National Conference on Computational Linguistics*, pages 600–610, 2023.
- [26] Seongyun Lee, Sue Hyun Park, Yongrae Jo, and Minjoon Seo. Volcano: Mitigating Multimodal Hallucination through Self-Feedback Guided Revision. In *Proceedings of the 2024 Conference of the North American Chapter of the Association for Computational Linguistics: Human Language Technologies (Volume 1: Long Papers)*, pages 391–404, 2024.
- [27] Sicong Leng, Hang Zhang, Guanzheng Chen, Xin Li, Shijian Lu, Chunyan Miao, and Lidong Bing. Mitigating Object Hallucinations in Large Vision-Language Models through Visual Contrastive Decoding. In *Proceedings of the IEEE/CVF Conference on Computer Vision and Pattern Recognition*, pages 13872–13882, 2024.
- [28] Aishwarya Agrawal, Dhruv Batra, and Devi Parikh. Analyzing the Behavior of Visual Question Answering Models. In *Proceedings of the 2016 conference on empirical methods in natural language processing*, pages 1955–1960, 2016.
- [29] Yash Goyal, Tejas Khot, Douglas Summers-Stay, Dhruv Batra, and Devi Parikh. Making the V in VQA Matter: Elevating the Role of Image Understanding in Visual Question Answering. In *Proceedings of the IEEE conference on computer vision and pattern recognition*, pages 6904–6913, 2017.
- [30] Vedika Agarwal, Rakshith Shetty, and Mario Fritz. Towards Causal VQA: Revealing and Reducing Spurious Correlations by Invariant and Covariant Semantic Editing. In *Proceedings of the IEEE/CVF Conference on Computer Vision and Pattern Recognition*, pages 9690–9698, 2020.
- [31] Yiyang Huang, Liang Shi, Yitian Zhang, Yi Xu, and Yun Fu. SHIELD: Suppressing Hallucinations In LVLm Encoders via Bias and Vulnerability Defense. *arXiv preprint arXiv:2510.16596*, 2025.
- [32] Zhiyuan Zhao, Bin Wang, Linke Ouyang, Xiaoyi Dong, Jiaqi Wang, and Conghui He. Beyond Hallucinations: Enhancing LVLms through Hallucination-Aware Direct Preference Optimization. *arXiv preprint arXiv:2311.16839*, 2023.
- [33] Shangpin Peng, Senqiao Yang, Li Jiang, and Zhuotao Tian. Mitigating Object Hallucinations via Sentence-Level Early Intervention. In *Proceedings of the IEEE/CVF International Conference on Computer Vision*, pages 635–646, 2025.

- [34] Zhihe Yang, Xufang Luo, Dongqi Han, Yunjian Xu, and Dongsheng Li. Mitigating Hallucinations in Large Vision-Language Models via DPO: On-Policy Data Hold the Key. *arXiv preprint arXiv:2501.09695*, 2025.
- [35] Rafael Rafailov, Archit Sharma, Eric Mitchell, Christopher D Manning, Stefano Ermon, and Chelsea Finn. Direct Preference Optimization: Your Language Model is Secretly a Reward Model. *Advances in neural information processing systems*, 36:53728–53741, 2023.
- [36] Daniel M Ziegler, Nisan Stiennon, Jeffrey Wu, Tom B Brown, Alec Radford, Dario Amodei, Paul Christiano, and Geoffrey Irving. Fine-Tuning Language Models from Human Preferences. *arXiv preprint arXiv:1909.08593*, 2019.
- [37] Nisan Stiennon, Long Ouyang, Jeffrey Wu, Daniel Ziegler, Ryan Lowe, Chelsea Voss, Alec Radford, Dario Amodei, and Paul F Christiano. Learning to summarize from human feedback. *Advances in neural information processing systems*, 33:3008–3021, 2020.
- [38] Long Ouyang, Jeffrey Wu, Xu Jiang, Diogo Almeida, Carroll Wainwright, Pamela Mishkin, Chong Zhang, Sandhini Agarwal, Katarina Slama, Alex Ray, et al. Training language models to follow instructions with human feedback. *Advances in neural information processing systems*, 35:27730–27744, 2022.
- [39] Yuntao Bai, Andy Jones, Kamal Ndousse, Amanda Askell, Anna Chen, Nova DasSarma, Dawn Drain, Stanislav Fort, Deep Ganguli, Tom Henighan, et al. Training a Helpful and Harmless Assistant with Reinforcement Learning from Human Feedback. *arXiv preprint arXiv:2204.05862*, 2022.
- [40] Zhiqing Sun, Sheng Shen, Shengcao Cao, Haotian Liu, Chunyuan Li, Yikang Shen, Chuang Gan, Liangyan Gui, Yu-Xiong Wang, Yiming Yang, et al. Aligning Large Multimodal Models with Factually Augmented RLHF. In *Findings of the Association for Computational Linguistics: ACL 2024*, pages 13088–13110, 2024.
- [41] Stephen Casper, Xander Davies, Claudia Shi, Thomas Krendl Gilbert, Jérémy Scheurer, Javier Rando, Rachel Freedman, Tomasz Korbak, David Lindner, Pedro Freire, et al. Open Problems and Fundamental Limitations of Reinforcement Learning from Human Feedback. *arXiv preprint arXiv:2307.15217*, 2023.
- [42] Hakim Sidahmed, Samrat Phatale, Alex Hutcheson, Zhuonan Lin, Zhang Chen, Zac Yu, Jarvis Jin, Simral Chaudhary, Roman Komarytsia, Christiane Ahlheim, et al. Parameter Efficient Reinforcement Learning from Human Feedback. *arXiv preprint arXiv:2403.10704*, 2024.
- [43] Long-Fei Li, Yu-Yang Qian, Peng Zhao, and Zhi-Hua Zhou. Provably Efficient Online RLHF with One-Pass Reward Modeling. *arXiv preprint arXiv:2502.07193*, 2025.
- [44] Hamish Ivison, Yizhong Wang, Jiacheng Liu, Zeqiu Wu, Valentina Pyatkin, Nathan Lambert, Noah A Smith, Yejin Choi, and Hannaneh Hajishirzi. Unpacking DPO and PPO: Disentangling Best Practices for Learning from Preference Feedback. *Advances in neural information processing systems*, 37:36602–36633, 2024.
- [45] Yu Pan, Zhongze Cai, Guanting Chen, Huaiyang Zhong, and Chonghuan Wang. What Matters in Data for DPO? *arXiv preprint arXiv:2508.18312*, 2025.
- [46] Yiyang Zhou, Chenhang Cui, Rafael Rafailov, Chelsea Finn, and Huaxiu Yao. Aligning Modalities in Vision Large Language Models via Preference Fine-tuning. *arXiv preprint arXiv:2402.11411*, 2024.
- [47] Pritam Sarkar, Sayna Ebrahimi, Ali Etemad, Ahmad Beirami, Sercan Ö. Arık, and Tomas Pfister. Mitigating Object Hallucination in MLLMs via Data-augmented Phrase-level Alignment, 2024.
- [48] Wenyi Xiao, Ziwei Huang, Leilei Gan, Wanggui He, Haoyuan Li, Zhelun Yu, Fangxun Shu, Hao Jiang, and Linchao Zhu. Detecting and Mitigating Hallucination in Large Vision Language Models via Fine-Grained AI Feedback. In *Proceedings of the AAAI Conference on Artificial Intelligence*, volume 39, pages 25543–25551, 2025.
- [49] Tianyu Yu, Haoye Zhang, Yuan Yao, Yunkai Dang, Da Chen, Xiaoman Lu, Ganqu Cui, Taiwen He, Zhiyuan Liu, Tat-Seng Chua, et al. RLAI-F-V: Aligning MLLMs through Open-Source AI Feedback for Super GPT-4V Trustworthiness. *arXiv preprint arXiv:2405.17220*, 2(3):8, 2024.
- [50] Rishabh Agarwal, Nino Vieillard, Yongchao Zhou, Piotr Stanczyk, Sabela Ramos Garea, Matthieu Geist, and Olivier Bachem. On-Policy Distillation of Language Models: Learning from Self-Generated Mistakes. In *The twelfth international conference on learning representations*, 2024.

- [51] Zhaorui Yang, Tianyu Pang, Haozhe Feng, Han Wang, Wei Chen, Minfeng Zhu, and Qian Liu. Self-Distillation Bridges Distribution Gap in Language Model Fine-Tuning. In *Proceedings of the 62nd Annual Meeting of the Association for Computational Linguistics (Volume 1: Long Papers)*, pages 1028–1043, 2024.
- [52] Siyan Zhao, Zhihui Xie, Mengchen Liu, Jing Huang, Guan Pang, Feiyu Chen, and Aditya Grover. Self-Distilled Reasoner: On-Policy Self-Distillation for Large Language Models. *arXiv preprint arXiv:2601.18734*, 2026.
- [53] John Schulman, Filip Wolski, Prafulla Dhariwal, Alec Radford, and Oleg Klimov. Proximal Policy Optimization Algorithms. *arXiv preprint arXiv:1707.06347*, 2017.
- [54] Yuntao Bai, Saurav Kadavath, Sandipan Kundu, Amanda Askell, Jackson Kernion, Andy Jones, Anna Chen, Anna Goldie, Azalia Mirhoseini, Cameron McKinnon, et al. Constitutional AI: Harmlessness from AI Feedback. *arXiv preprint arXiv:2212.08073*, 2022.
- [55] Zhihong Shao, Peiyi Wang, Qihao Zhu, Runxin Xu, Junxiao Song, Xiao Bi, Haowei Zhang, Mingchuan Zhang, YK Li, Yang Wu, et al. DeepSeekMath: Pushing the Limits of Mathematical Reasoning in Open Language Models. *arXiv preprint arXiv:2402.03300*, 2024.
- [56] Yao Zhao, Rishabh Joshi, Tianqi Liu, Misha Khalman, Mohammad Saleh, and Peter J Liu. SLiC-HF: Sequence Likelihood Calibration with Human Feedback. *arXiv preprint arXiv:2305.10425*, 2023.
- [57] Mohammad Gheshlaghi Azar, Zhaohan Daniel Guo, Bilal Piot, Remi Munos, Mark Rowland, Michal Valko, and Daniele Calandriello. A General Theoretical Paradigm to Understand Learning from Human Preferences. In *International Conference on Artificial Intelligence and Statistics*, pages 4447–4455. PMLR, 2024.
- [58] Kawin Ethayarajh, Winnie Xu, Niklas Muennighoff, Dan Jurafsky, and Douwe Kiela. KTO: Model Alignment as Prospect Theoretic Optimization. *arXiv preprint arXiv:2402.01306*, 2024.
- [59] Jiwoo Hong, Noah Lee, and James Thorne. ORPO: Monolithic Preference Optimization without Reference Model. In *Proceedings of the 2024 Conference on Empirical Methods in Natural Language Processing*, pages 11170–11189, 2024.
- [60] Yu Meng, Mengzhou Xia, and Danqi Chen. SimPO: Simple Preference Optimization with a Reference-Free Reward. *Advances in Neural Information Processing Systems*, 37:124198–124235, 2024.
- [61] Yuxi Xie, Guanzhen Li, Xiao Xu, and Min-Yen Kan. V-DPO: Mitigating Hallucination in Large Vision Language Models via Vision-Guided Direct Preference Optimization. In *Findings of the Association for Computational Linguistics: EMNLP 2024*, pages 13258–13273, 2024.
- [62] Songtao Jiang, Yan Zhang, Ruizhe Chen, Tianxiang Hu, Yeying Jin, Qinglin He, Yang Feng, Jian Wu, and Zuozhu Liu. Modality-Fair Preference Optimization for Trustworthy MLLM Alignment. *arXiv preprint arXiv:2410.15334*, 2024.
- [63] Fei Wang, Wenxuan Zhou, James Y Huang, Nan Xu, Sheng Zhang, Hoifung Poon, and Muhao Chen. mDPO: Conditional Preference Optimization for Multimodal Large Language Models. In *Proceedings of the 2024 Conference on Empirical Methods in Natural Language Processing*, pages 8078–8088, 2024.
- [64] Wenqi Liu, Xuemeng Song, Jiaxi Li, Yinwei Wei, Na Zheng, Jianhua Yin, and Liqiang Nie. Mitigating Hallucination Through Theory-Consistent Symmetric Multimodal Preference Optimization. *arXiv preprint arXiv:2506.11712*, 2025.
- [65] Tianyu Yu, Yuan Yao, Haoye Zhang, Taiwan He, Yifeng Han, Ganqu Cui, Jinyi Hu, Zhiyuan Liu, Hai-Tao Zheng, Maosong Sun, et al. RLHF-V: Towards Trustworthy MLLMs via Behavior Alignment from Fine-grained Correctional Human Feedback. In *Proceedings of the IEEE/CVF Conference on Computer Vision and Pattern Recognition*, pages 13807–13816, 2024.
- [66] Lehan He, Zeren Chen, Zhelun Shi, Tianyu Yu, Jing Shao, and Lu Sheng. Systematic Reward Gap Optimization for Mitigating VLM Hallucinations. *arXiv preprint arXiv:2411.17265*, 2024.
- [67] Renjie Pi, Tianyang Han, Wei Xiong, Jipeng Zhang, Runtao Liu, Rui Pan, and Tong Zhang. Strengthening Multimodal Large Language Model with Bootstrapped Preference Optimization. In *European Conference on Computer Vision*, pages 382–398. Springer, 2024.
- [68] Shilong Liu, Zhaoyang Zeng, Tianhe Ren, Feng Li, Hao Zhang, Jie Yang, Qing Jiang, Chunyuan Li, Jianwei Yang, Hang Su, et al. Grounding DINO: Marrying DINO with Grounded Pre-Training for Open-Set Object Detection. In *European conference on computer vision*, pages 38–55. Springer, 2024.

- [69] Tianheng Cheng, Lin Song, Yixiao Ge, Wenyu Liu, Xinggang Wang, and Ying Shan. YOLO-World: Real-Time Open-Vocabulary Object Detection. In *Proceedings of the IEEE/CVF conference on computer vision and pattern recognition*, pages 16901–16911, 2024.
- [70] Fahim Tajwar, Anikait Singh, Archit Sharma, Rafael Rafailov, Jeff Schneider, Tengyang Xie, Stefano Ermon, Chelsea Finn, and Aviral Kumar. Preference Fine-Tuning of LLMs Should Leverage Suboptimal, On-Policy Data. *arXiv preprint arXiv:2404.14367*, 2024.
- [71] Yizhong Wang, Yeganeh Kordi, Swaroop Mishra, Alisa Liu, Noah A Smith, Daniel Khoshabi, and Hannaneh Hajishirzi. Self-instruct: Aligning language models with self-generated instructions. In *Proceedings of the 61st annual meeting of the association for computational linguistics (volume 1: long papers)*, pages 13484–13508, 2023.
- [72] Weizhe Yuan, Richard Yuanzhe Pang, Kyunghyun Cho, Xian Li, Sainbayar Sukhbaatar, Jing Xu, and Jason Weston. Self-Rewarding Language Models. *arXiv preprint arXiv:2401.10020*, 2024.
- [73] Yue Wu, Zhiqing Sun, Huizhuo Yuan, Kaixuan Ji, Yiming Yang, and Quanquan Gu. Self-Play Preference Optimization for Language Model Alignment. *arXiv preprint arXiv:2405.00675*, 2024.
- [74] Qingxiu Dong, Li Dong, Xingxing Zhang, Zhifang Sui, and Furu Wei. Self-Boosting Large Language Models with Synthetic Preference Data. *arXiv preprint arXiv:2410.06961*, 2024.
- [75] Yung-Sung Chuang, Yujia Xie, Hongyin Luo, Yoon Kim, James Glass, and Pengcheng He. DoLa: Decoding by Contrasting Layers Improves Factuality in Large Language Models. *arXiv preprint arXiv:2309.03883*, 2023.
- [76] Qidong Huang, Xiaoyi Dong, Pan Zhang, Bin Wang, Conghui He, Jiaqi Wang, Dahua Lin, Weiming Zhang, and Nenghai Yu. OPERA: Alleviating Hallucination in Multi-Modal Large Language Models via Over-Trust Penalty and Retrospection-Allocation. In *Proceedings of the IEEE/CVF Conference on Computer Vision and Pattern Recognition*, pages 13418–13427, 2024.
- [77] Shangyu Xing, Fei Zhao, Zhen Wu, Tuo An, Weihao Chen, Chunhui Li, Jianbing Zhang, and Xinyu Dai. EFUF: Efficient Fine-grained Unlearning Framework for Mitigating Hallucinations in Multimodal Large Language Models. In *Proceedings of the 2024 Conference on Empirical Methods in Natural Language Processing*, pages 1167–1181, 2024.
- [78] Qwen Team. Qwen2.5-VL, January 2025. URL <https://qwenlm.github.io/blog/qwen2.5-vl/>.
- [79] Patrick Esser, Sumith Kulal, Andreas Blattmann, Rahim Entezari, Jonas Müller, Harry Saini, Yam Levi, Dominik Lorenz, Axel Sauer, Frederic Boesel, et al. Scaling Rectified Flow Transformers for High-Resolution Image Synthesis. In *Forty-first international conference on machine learning*, 2024.
- [80] Weiyun Wang, Zhangwei Gao, Lixin Gu, Hengjun Pu, Long Cui, Xingguang Wei, Zhaoyang Liu, Linglin Jing, Shenglong Ye, Jie Shao, et al. InternVL3.5: Advancing Open-Source Multimodal Models in Versatility, Reasoning, and Efficiency. *arXiv preprint arXiv:2508.18265*, 2025.
- [81] Jiabo Ye, Haiyang Xu, Haowei Liu, Anwen Hu, Ming Yan, Qi Qian, Ji Zhang, Fei Huang, and Jingren Zhou. mPLUG-Owl3: Towards Long Image-Sequence Understanding in Multi-Modal Large Language Models. *arXiv preprint arXiv:2408.04840*, 2024.
- [82] Kimi Team, Angang Du, Bohong Yin, Bowei Xing, Bowen Qu, Bowen Wang, Cheng Chen, Chenlin Zhang, Chenzhuang Du, Chu Wei, Congcong Wang, Dehao Zhang, Dikang Du, Dongliang Wang, Enming Yuan, Enzhe Lu, Fang Li, Flood Sung, Guangda Wei, Guokun Lai, Han Zhu, Hao Ding, Hao Hu, Hao Yang, Hao Zhang, Haoning Wu, Haotian Yao, Haoyu Lu, Heng Wang, Hongcheng Gao, Huabin Zheng, Jiaming Li, Jianlin Su, Jianzhou Wang, Jiaqi Deng, Jiezhong Qiu, Jin Xie, Jinhong Wang, Jingyuan Liu, Junjie Yan, Kun Ouyang, Liang Chen, Lin Sui, Longhui Yu, Mengfan Dong, Mengnan Dong, Nuo Xu, Pengyu Cheng, Qizheng Gu, Runjie Zhou, Shaowei Liu, Sihan Cao, Tao Yu, Tianhui Song, Tongtong Bai, Wei Song, Weiran He, Weixiao Huang, Weixin Xu, Xiaokun Yuan, Xingcheng Yao, Xingzhe Wu, Xinxing Zu, Xinyu Zhou, Xinyuan Wang, Y. Charles, Yan Zhong, Yang Li, Yangyang Hu, Yanru Chen, Yejie Wang, Yibo Liu, Yibo Miao, Yidao Qin, Yimin Chen, Yiping Bao, Yiqin Wang, Yongsheng Kang, Yuanxin Liu, Yulun Du, Yuxin Wu, Yuzhi Wang, Yuzi Yan, Zaida Zhou, Zhaowei Li, Zhejun Jiang, Zheng Zhang, Zhilin Yang, Zhiqi Huang, Zihao Huang, Zijia Zhao, and Ziwei Chen. Kimi-VL Technical Report, 2025. URL <https://arxiv.org/abs/2504.07491>.
- [83] Aaditya Singh, Adam Fry, Adam Perelman, Adam Tart, Adi Ganesh, Ahmed El-Kishky, Aidan McLaughlin, Aiden Low, AJ Ostrow, Akhila Ananthram, et al. OpenAI GPT-5 System Card. *arXiv preprint arXiv:2601.03267*, 2025.

- [84] Black Forest Labs. FLUX. <https://github.com/black-forest-labs/flux>, 2024.
- [85] Yongsheng Yu, Wei Xiong, Weili Nie, Yichen Sheng, Shiqiu Liu, and Jiebo Luo. PixelDiT: Pixel Diffusion Transformers for Image Generation. *arXiv preprint arXiv:2511.20645*, 2025.
- [86] Ranjay Krishna, Yuke Zhu, Oliver Groth, Justin Johnson, Kenji Hata, Joshua Kravitz, Stephanie Chen, Yannis Kalantidis, Li-Jia Li, David A Shamma, et al. Visual Genome: Connecting Language and Vision Using Crowdsourced Dense Image Annotations. *International journal of computer vision*, 123(1):32–73, 2017.
- [87] Anna Rohrbach, Lisa Anne Hendricks, Kaylee Burns, Trevor Darrell, and Kate Saenko. Object Hallucination in Image Captioning. In *Proceedings of the 2018 Conference on Empirical Methods in Natural Language Processing*, pages 4035–4045, 2018.
- [88] Junyang Wang, Yuhang Wang, Guohai Xu, Jing Zhang, Yukai Gu, Haitao Jia, Jiaqi Wang, Haiyang Xu, Ming Yan, Ji Zhang, et al. AMBER: An LLM-free Multi-dimensional Benchmark for MLLMs Hallucination Evaluation. *arXiv preprint arXiv:2311.07397*, 2023.
- [89] Lin Chen, Jinsong Li, Xiaoyi Dong, Pan Zhang, Yuhang Zang, Zehui Chen, Haodong Duan, Jiaqi Wang, Yu Qiao, Dahua Lin, et al. Are We on the Right Way for Evaluating Large Vision-Language Models? *Advances in Neural Information Processing Systems*, 37:27056–27087, 2024.
- [90] Shengbang Tong, Zhuang Liu, Yuexiang Zhai, Yi Ma, Yann LeCun, and Saining Xie. Eyes Wide Shut? Exploring the Visual Shortcomings of Multimodal LLMs. In *Proceedings of the IEEE/CVF conference on computer vision and pattern recognition*, pages 9568–9578, 2024.
- [91] Shengbang Tong, Ellis Brown, Penghao Wu, Sanghyun Woo, Manoj Middepogu, Sai C Akula, Jihan Yang, Shusheng Yang, Adithya Iyer, Xichen Pan, et al. Cambrian-1: A Fully Open, Vision-Centric Exploration of Multimodal LLMs. *Advances in Neural Information Processing Systems*, 37:87310–87356, 2024.
- [92] Olga Russakovsky, Jia Deng, Hao Su, Jonathan Krause, Sanjeev Satheesh, Sean Ma, Zhiheng Huang, Andrej Karpathy, Aditya Khosla, Michael Bernstein, Alexander C. Berg, and Li Fei-Fei. ImageNet Large Scale Visual Recognition Challenge. *International Journal of Computer Vision (IJCV)*, 115(3):211–252, 2015. doi: 10.1007/s11263-015-0816-y.
- [93] Dan Hendrycks, Kevin Zhao, Steven Basart, Jacob Steinhardt, and Dawn Song. Natural Adversarial Examples. *CVPR*, 2021.
- [94] Richard Socher, Alex Perelygin, Jean Wu, Jason Chuang, Christopher D Manning, Andrew Y Ng, and Christopher Potts. Recursive Deep Models for Semantic Compositionality Over a Sentiment Treebank. In *Proceedings of the 2013 conference on empirical methods in natural language processing*, pages 1631–1642, 2013.
- [95] Tsung-Yi Lin, Michael Maire, Serge Belongie, James Hays, Pietro Perona, Deva Ramanan, Piotr Dollár, and C Lawrence Zitnick. Microsoft COCO: Common Objects in Context. In *European conference on computer vision*, pages 740–755. Springer, 2014.
- [96] Ziyu Liu, Zeyi Sun, Yuhang Zang, Xiaoyi Dong, Yuhang Cao, Haodong Duan, Dahua Lin, and Jiaqi Wang. Visual-RFT: Visual Reinforcement Fine-Tuning. In *Proceedings of the IEEE/CVF International Conference on Computer Vision*, pages 2034–2044, 2025.
- [97] Ian Covert, Tony Sun, James Zou, and Tatsunori Hashimoto. Locality Alignment Improves Vision-Language Models. *arXiv preprint arXiv:2410.11087*, 2024.
- [98] Wan Team. Wan: Open and Advanced Large-Scale Video Generative Models, 2025.
- [99] Bolei Zhou, Hang Zhao, Xavier Puig, Sanja Fidler, Adela Barriuso, and Antonio Torralba. Scene Parsing through ADE20K Dataset. In *Proceedings of the IEEE conference on computer vision and pattern recognition*, pages 633–641, 2017.
- [100] Garrick Brazil, Abhinav Kumar, Julian Straub, Nikhila Ravi, Justin Johnson, and Georgia Gkioxari. Omni3D: A Large Benchmark and Model for 3D Object Detection in the Wild. In *Proceedings of the IEEE/CVF conference on computer vision and pattern recognition*, pages 13154–13164, 2023.

A Limitations and broader impact

Although ViPSy achieves strong hallucination mitigation, it relies on external models for preference construction, including a text-to-image diffusion model and a judge VLM. Consequently, the resulting preference pairs may inherit biases or failure modes from these models when synthesized variants or judge decisions do not faithfully reflect image-grounded evidence. Improving or domain-adapting these external models could further enhance preference quality. This study also focuses mainly on object-level visual grounding with cues from Visual Genome images. While effective for reducing object hallucination, broader scenarios such as complex reasoning, spatial understanding, and specialized domains remain underexplored. ViPSy may improve VLM reliability in applications such as education, accessibility, robotics, industrial inspection, and assistive scientific or medical workflows.

B Training details

We build our experiments on top of LLaVA-1.5 [1], using Vicuna-1.5 [8] as the language model backbone and CLIP ViT-L/336px [6] as the vision encoder. The visual features are mapped to the language space through the default two-layer GELU MLP projector. The training set is constructed from Visual Genome images [86]. Our final preference dataset contains 7K preference pairs, which is smaller than the training data used by Peng et al. [33], the previous state-of-the-art method for hallucination mitigation. This allows us to evaluate whether visually grounded preference construction can be effective even with a relatively compact preference dataset. For optimization, we use LoRA-based parameter-efficient tuning. The tuning targets include the LLM, the vision encoder, and the projector. We insert trainable LoRA modules into these components rather than updating all model parameters. The LoRA modules for the LLM and projector are trained with a learning rate of 2×10^{-5} , while the vision encoder uses 2×10^{-6} . We use LoRA rank $r = 128$, scaling factor $\alpha = 256$, and set the preference loss coefficient to $\beta = 0.1$. Models are trained with AdamW, cosine learning-rate decay, no weight decay, and a maximum context length of 2048. Training is performed for one epoch with a global batch size of 64. We employ ZeRO stage-2 optimization to reduce memory usage. Both N_c and N_s are set to 8, representing the number of captions and cue-conditioned self-generated candidates, respectively.

Compute infrastructure.

All experiments were conducted on compute cluster instances with two NVIDIA B200 GPUs, each with 183GB of VRAM, two Intel Xeon 6960P CPUs with 144 physical cores and 288 threads in total.

C Models

Policy Models.

- **LLaVA 1.5** [1] is used as the main policy model in our experiments. We evaluate both the 7B and 13B variants to study the effect of policy model scale. LLaVA 1.5 combines a CLIP-based visual encoder with a Vicuna language model through a multimodal projector, enabling it to generate language responses conditioned on both images and textual instructions. In our framework, LLaVA 1.5 generates self-captions, produces cue-conditioned candidate responses, and is optimized with the preference pairs constructed by ViPSy. Its relatively simple connector-based design also makes it a useful baseline for isolating how preference optimization, rather than architectural complexity, affects visual grounding behavior.
- **InternVL3.5-8B** [80] is used as an additional policy model to evaluate whether ViPSy generalizes beyond the LLaVA family. InternVL3.5 is a multimodal instruction-following model designed for visual understanding and reasoning. Including this model allows us to test whether visually grounded preference construction remains effective for a different VLM architecture.
- **Kimi-VL-A3B** [82] is used as a policy model for evaluating generalization across model families. It is a vision-language model developed for multimodal instruction following and image-grounded reasoning. This model is included to evaluate whether ViPSy improves visual grounding when applied to a policy model with a distinct multimodal architecture.

- **mPLUG-Owl3-7B** [81] is used as another policy model in our policy generalization experiments. The mPLUG-Owl family follows a modular multimodal design that connects visual perception with language generation. We include this model to examine whether ViPSy can improve visual grounding for a policy model with a different multimodal architecture.
- **Qwen2.5-VL-7B** [78] is used as a policy model in addition to its larger judge counterpart. It is an instruction-tuned vision-language model with strong visual understanding and multimodal reasoning capabilities. Using the 7B variant as a policy model helps evaluate whether ViPSy is effective for a compact Qwen-family VLM, rather than only for LLaVA-based policies.

Judge Models.

- **Qwen2.5-VL-72B** [78] is used as the default judge model in our experiments. We use this model to extract consistent visual cues between original and synthetic images and to select preferred and dispreferred responses from cue-conditioned candidates. Due to its large scale and instruction-tuned multimodal capability, it provides a strong visual understanding for evaluating whether a response is grounded in the original image. Its fine-grained visual localization capability is useful for judging whether candidate responses preserve object- and region-level evidence rather than only global image semantics.
- **Qwen3-VL-30B** [4] is used as a judge model. It serves as an alternative multimodal evaluator for cue extraction and preference selection, allowing us to examine whether ViPSy depends on a single judge architecture. By including Qwen3-VL-30B, we assess the robustness of the constructed preferences across different VLM judges. In our experiments, Qwen3-VL-30B is used only for judging and not as the policy model being optimized.
- **GPT-5 mini** [83] is used as an additional judge model for cue extraction and preference selection. We include it as a complementary evaluator to the Qwen-family VLM judges, allowing us to examine whether preference construction remains robust when the judge comes from a different model family. In our experiments, GPT-5 mini is used only for judging and not as the policy model being optimized. As a lightweight text-and-vision model, it provides a cost-efficient contrast to larger VLM judges while retaining multimodal reasoning ability for preference selection.

Text-to-Image Models.

- **SD-3.5** [79] is included as a representative latent-space diffusion model. It generates images in a compressed latent representation rather than directly in pixel space, which enables efficient image synthesis while maintaining high visual quality. In our experiments, SD-3.5-L is used to synthesize semantically aligned image variants for visual cue extraction. Its multimodal transformer backbone enables strong interaction between text and image representations, making it a reliable latent-generation baseline for cue-consistency analysis.
- **Flux-1.0-dev** [84] is included as a representative flow matching model. Unlike standard denoising diffusion formulations, flow matching learns a continuous transformation from noise to data. We use Flux-1.0-dev to test whether ViPSy is robust to a different text-to-image generation paradigm during semantic synthesis. As a high-capacity rectified-flow transformer trained with guidance distillation, it provides a distinct synthesis backbone with strong prompt-following behavior.
- **PixelDiT** [85] is included as a representative pixel-space diffusion model. In contrast to latent diffusion models, PixelDiT performs generation in pixel space. We include PixelDiT to examine whether visual cue extraction remains effective with pixel-space diffusion.

D Baselines

We compare ViPSy with hallucination mitigation methods for VLMs. All baselines use LLaVA-1.5 to ensure a fair comparison. We organize the baselines into three groups: sampling-based methods, intervention-based methods, and other methods. Sampling-based methods construct preference data from VLM-generated responses, which keeps the data close to the policy distribution, but they can still underuse visual information. Intervention-based methods construct preference data through

external editing or correction, creating explicit contrasts between hallucinated and hallucination-free responses while moving the data away from the policy distribution. Other methods include one unlearning-based method and three training-free decoding methods.

Sampling-based methods.

- **LLaVA-RLHF** [40] learns a reward model from human feedback and uses reinforcement learning to train the VLM to prefer image-faithful responses. To better penalize hallucinations, the reward model is also given extra factual evidence, such as image captions or ground-truth answers.
- **RLAIF-V** [49] uses sampling-based AI feedback to reduce hallucinations in VLMs. It generates multiple candidate responses via controlled sampling under the same input, allowing preference pairs to focus on trustworthiness differences. It then scores responses at the claim level and iteratively refines the VLM using the resulting preference feedback.
- **SENTINEL** [33] targets object hallucination via sentence-level early intervention. It constructs in-domain preference pairs by using open-vocabulary object detectors to validate objects in VLM-generated sentences, and trains the VLM to prefer context-coherent non-hallucinated sentences over hallucinated ones, reducing hallucination propagation.
- **OPA-DPO** [34] performs on-policy alignment with corrected responses. It uses GPT-4V to minimally revise hallucinated VLM outputs and applies LoRA-SFT to align both ground-truth and revised responses with the VLM’s policy distribution.

Intervention-based methods.

- **HALVA** [47] addresses object hallucination in VLMs through Data-augmented Phrase-level Alignment (DPA). DPA constructs correct and hallucinated response pairs by selectively replacing grounded visual concepts in correct responses with hallucinated phrases. It penalizes hallucinated phrases relative to their correct counterparts, while using token-wise KL regularization to preserve general vision-language capabilities.
- **HA-DPO** [32] builds preference data from Visual Genome images by prompting VLMs to generate detailed descriptions and using GPT-4 with VG annotations to identify unsupported visual claims and revise them. The revised faithful responses are then paired with their original erroneous counterparts, producing positive and negative samples for preference-based training.
- **POVID** [46] frames VLM hallucination as modality misalignment and constructs preference pairs by keeping grounded responses as preferred while generating dispreferences through text- and image-side interventions. Text interventions inject plausible hallucinations, whereas image distortions trigger inherent hallucination patterns, guiding preference optimization toward visually grounded generation.
- **HSA-DPO** [48] trains a sentence-level hallucination detector from fine-grained AI feedback and uses it as a detect-then-rewrite intervention to build preference pairs.
- **TPR** [66] intervenes in preference data at the topic level. Through selective replacement with VLM-resampled topic alternatives, it controls reward gaps and applies curriculum hard negative mining for data-efficient alignment.

Other methods.

- **EFUF** [77] is an unlearning-based method for reducing object hallucinations in VLMs. It uses CLIP-based image-relevance scores to automatically curate grounded and hallucinated object mentions without paired annotations, then unlearns hallucinated subsentences while preserving correct object generation and sentence fluency.
- **VCD** [27] is a training-free decoding method based on visual contrastive decoding. It contrasts the output distributions conditioned on the original image and a noise-distorted visual input, thereby calibrating predictions that are overly driven by language priors and statistical biases rather than visual evidence.

- **DoLa** [75] is a training-free decoding method that improves factuality by contrasting predictions from earlier and later transformer layers during decoding. This helps the model rely on factual knowledge it has already learned, without using external retrieval or additional fine-tuning.
- **OPERA** [76] is a training-free decoding method that adjusts beam search based on self-attention patterns. It penalizes candidates that rely too much on summary tokens and, when this reliance leads to hallucination, revises the generation by returning to an earlier token and choosing a different next token.

E Data

E.1 Training data

We construct the VLM preference training data using images from Visual Genome (VG) [86]. VG is a large-scale vision-language dataset that provides dense annotations for real-world images, including region descriptions, objects, attributes, relationships, and question-answer pairs. We use VG images as source images to generate visual variations and extract consistent visual cues for preference construction. Since our method relies on diverse visual scenes for this process, VG serves as a suitable data source for applying the proposed method.

E.2 Evaluation data

We evaluate the VLM on two groups of benchmarks, namely hallucination benchmarks and general visual-language capabilities benchmarks. In addition, to examine whether the proposed training improves the underlying vision encoder, we conduct vision encoder evaluations using linear probing and segmentation datasets. For hallucination evaluation, we use Object HalBench, AMBER, and HallusionBench. For general multimodal evaluation, we use MMStar, MMVP, and CV-Bench. For vision encoder evaluation, we use ImageNet, ImageNet-O, Rendered-SST2, and MSCOCO.

E.2.1 Hallucination Benchmarks

- **Object HalBench** [87] is based on MSCOCO [95] and evaluates object hallucination in image captions. Evaluation is restricted to the 80 MSCOCO object categories with segmentation annotations. Object presence is determined using both MSCOCO segmentation labels and reference captions, and generated object mentions are normalized through singularization and synonym matching.

We report two hallucination metrics, Resp. and Ment. Resp. measures the fraction of generated responses that contain at least one hallucinated object, while Ment. measures the fraction of object mentions that are hallucinated:

$$\text{Resp.} = \frac{N_{\text{resp.}}^{\text{hal.}}}{N_{\text{resp.}}}, \quad \text{Ment.} = \frac{N_{\text{ment.}}^{\text{hal.}}}{N_{\text{ment.}}} \quad (8)$$

Here, $N_{\text{resp.}}$ is the total number of generated responses, and $N_{\text{resp.}}^{\text{hal.}}$ is the number of responses containing at least one hallucinated object. Similarly, $N_{\text{ment.}}$ is the total number of generated object mentions, and $N_{\text{ment.}}^{\text{hal.}}$ is the number of hallucinated object mentions. Lower values indicate less object hallucination.

- **AMBER** [88] contains 1,004 manually selected images annotated with visible objects, attributes, relations, and cognitively plausible hallucination target objects. We use its generative evaluation split, where models are prompted with “Describe this image.” and hallucination is evaluated from the generated image description.

Given a response R , noun mentions are extracted as candidate objects R_{obj} and filtered using the AMBER object vocabulary X_{obj} :

$$R'_{\text{obj}} = R_{\text{obj}} \cap X_{\text{obj}} \quad (9)$$

The filtered object mentions R'_{obj} , which are then compared with the ground-truth object set A_{obj} , and the hallucination target set H_{obj} . We report three metrics: CHAIR, Hal., and Cog.

CHAIR measures the fraction of generated object mentions ungrounded in the image:

$$\text{CHAIR}(R) = 1 - \frac{|R'_{\text{obj}} \cap A_{\text{obj}}|}{|R'_{\text{obj}}|}. \quad (10)$$

Hal. is a response-level hallucination indicator that checks whether the response contains at least one ungrounded object:

$$\text{Hal}(R) = \mathbb{I}[\text{CHAIR}(R) \neq 0]. \quad (11)$$

Cog. measures the fraction of generated object mentions that match AMBER’s cognitively plausible hallucination targets, i.e., absent objects that are likely to be imagined from the visual context:

$$\text{Cog}(R) = \frac{|R'_{\text{obj}} \cap H_{\text{obj}}|}{|R'_{\text{obj}}|}. \quad (12)$$

All three metrics are averaged over the generative-evaluation samples, and lower values indicate better performance.

- **HallusionBench** [22] evaluates image-context reasoning in VLMs, focusing on language hallucination and visual illusion. It consists of 346 images and 1,129 human-crafted yes/no questions across diverse visual formats, including charts, tables, maps, OCR images, optical illusions, math figures, posters, and video-like image sequences.

We report the overall question-level accuracy, denoted as All Acc. (aAcc). For each valid image-question pair (\mathbf{I}, \mathbf{q}) , the model prediction is mapped to a binary correctness value $b_M(\mathbf{I}, \mathbf{q}) \in \{0, 1\}$, where 1 indicates a correct prediction, and 0 indicates an incorrect prediction. The metric is computed as the average correctness over all valid pairs:

$$\text{aAcc} = \frac{\sum_{(\mathbf{I}, \mathbf{q}) \in \mathcal{V}} b_M(\mathbf{I}, \mathbf{q})}{|\mathcal{V}|}. \quad (13)$$

Here, \mathcal{V} is the set of valid image-question pairs. Higher values indicate better performance.

E.2.2 General benchmarks

- **MMStar** [89] is a vision-indispensable multimodal benchmark consisting of 1,500 human-curated samples across 6 core capabilities and 18 fine-grained axes. It evaluates the visual understanding and reasoning abilities of large vision-language models across coarse perception, fine-grained perception, instance reasoning, logical reasoning, science and technology, and mathematics. The benchmark is designed to reduce text-only shortcuts and data leakage by requiring models to rely on visual content to answer each question.
- **MMVP** [90] evaluates the fine-grained visual grounding ability of multimodal LLMs through visual question answering on CLIP-blind image pairs. These image pairs are visually different to humans but are encoded similarly by CLIP, making them useful for testing whether a model can recognize subtle visual details. The benchmark covers basic visual patterns, including orientation and direction, presence of specific features, state and condition, counting, positional relationships, color and appearance, structural characteristics, text, and viewpoint. Following the official evaluation protocol, an image pair is counted as correct only when both associated questions are answered correctly.
- **CV-Bench** [91] is a vision-centric benchmark for evaluating the fundamental visual understanding capabilities of multimodal LLMs. It reformulates standard computer vision benchmarks into VQA-style questions to assess both 2D and 3D perception. The 2D tasks evaluate spatial relationships and object counting, while the 3D tasks evaluate depth order and relative distance. The benchmark contains 2,638 manually inspected examples constructed from ADE20K [99], MSCOCO [95], and Omni3D [100]. For CV-Bench, Acc. is computed as the average accuracy over the 2D and 3D task groups.

Algorithm 1 ViPSy

Input: Dataset $\mathcal{D} = \{(\mathbf{x}_i, \mathbf{m}_i)\}_{i=1}^M$; policy π_θ ; judge π_ϕ ; T2I model P_ψ ; number of self-captions/synthetic variants N_c ; number of cue-conditioned rollouts N_s ; prompts \mathbf{x}_{cap} for captioning, \mathbf{x}_{comp} for image comparison, \mathbf{x}_{agg} for cue aggregation, $\mathbf{x}_{\text{cue-cap}}$ for cue-conditioned rollout, and \mathbf{x}_{vis} for visual-grounding preference selection

Output: Preference dataset $\mathcal{D}_{\text{pref}}$

```
1:  $\mathcal{D}_{\text{pref}} \leftarrow \emptyset$  // Initialize preference dataset
2: for each  $(\mathbf{x}_i, \mathbf{m}_i) \in \mathcal{D}$  do
  {Stage 1: Self-captioned visual cue extraction}
3:  $\{\mathbf{q}_j\}_{j=1}^{N_c} \sim \pi_\theta(\cdot | \mathbf{x}_{\text{cap}}, \mathbf{m}_i)$  // Generate  $N_c$  self-captions
4:  $\{\mathbf{m}'_{i,j}\}_{j=1}^{N_c} = \{P_\psi(\mathbf{q}_j)\}_{j=1}^{N_c}$  // Synthesize semantic image variants
5:  $\mathbf{c}_{i,j} = \pi_\phi(\mathbf{x}_{\text{comp}}, \mathbf{m}_i, \mathbf{m}'_{i,j})$  // Extract consistent visual cues
6:  $\mathbf{c}_i = \pi_\phi(\mathbf{x}_{\text{agg}}, \{\mathbf{c}_{i,j}\}_{j=1}^{N_c})$  // Aggregate consistent visual cues
  {Stage 2: Cue-conditioned preference synthesis}
7:  $\mathbf{y}_i^{(s)} \sim \pi_\theta(\cdot | \mathbf{x}_{\text{cue-cap}}, \mathbf{m}_i, \mathbf{c}_i)$ ,  $s = 1, \dots, N_s$  // Sample cue-conditioned responses
8:  $(\mathbf{y}_{w,i}, \mathbf{y}_{l,i}) = \pi_\phi(\mathbf{x}_{\text{vis}}, \mathbf{m}_i, \{\mathbf{y}_i^{(s)}\}_{s=1}^{N_s})$  // Select visually grounded and less grounded responses
9:  $\mathcal{D}_{\text{pref}} \leftarrow \mathcal{D}_{\text{pref}} \cup \{(\mathbf{x}_i, \mathbf{m}_i, \mathbf{y}_{w,i}, \mathbf{y}_{l,i})\}$  // Store preference pair
10: end for
11: return  $\mathcal{D}_{\text{pref}}$ 
```

E.2.3 Vision encoder evaluation

- **ImageNet-1k** [92] is a large-scale object recognition benchmark with 1,000 semantic categories. We use ImageNet-1k to evaluate the global semantic representation quality of the vision encoder through linear probing, where the vision encoder is frozen, and only a data-specific linear classifier is trained on top of the extracted visual features. We report classification accuracy (Acc.), where higher values indicate better performance.
- **ImageNet-O** [93] is an out-of-distribution object recognition benchmark designed to evaluate model robustness beyond the ImageNet distribution. We use ImageNet-O to examine whether the learned visual representations remain effective on uncommon and challenging object-centric images. Since ImageNet-O is used in a few-shot evaluation setting, we select a small number of samples from its test set for few-shot training. Specifically, the vision encoder is frozen, and only a data-specific linear classifier is trained using the extracted visual features of the selected few-shot samples. We then evaluate the classifier on the remaining ImageNet-O test samples. This benchmark complements ImageNet-1k by evaluating whether visual features remain effective across diverse distributions. We report classification accuracy (Acc.), where higher values indicate better performance.
- **Rendered-SST2** [94, 6] is constructed by rendering sentences from the SST-2 sentiment classification dataset as images. We use Rendered-SST2 under the same linear-probing setting, where the vision encoder is frozen, and only a data-specific linear classifier is trained on top of the extracted visual features. This benchmark evaluates whether the vision encoder preserves semantic information in text-rendered visual inputs. Unlike object-centric recognition datasets, Rendered-SST2 tests whether visual representations can capture image-based textual semantics. We report classification accuracy (Acc.), where higher values indicate better performance.
- **MSCOCO** [95] contains images with object-level annotations, including segmentation masks. We use MSCOCO for segmentation evaluation to assess whether the vision encoder can distinguish fine-grained object-level information. This evaluation complements linear probing by measuring local visual grounding rather than only global image-level semantics. We report Recall, where higher values indicate better performance.

Table 6: Results on hallucination and general benchmarks using various policy models. We apply ViPSy to diverse policy models.

Method	Hallucination benchmarks						General benchmarks		
	Object HalBench [87]		AMBER [88]		Hal. Bench [22]		MMStar [89]	MMVP [90]	CV-Bench [91]
	Resp.↓	Ment.↓	CHAIR↓	Hal.↓	Cog.↓	aAcc.↑	Acc.↑	Acc.↑	Acc.↑
Qwen2.5-VL-7B									
Vanilla	9.0	5.3	5.0	26.4	1.7	57.7	59.8	56.6	78.3
ViPSy (Ours)	7.6	4.8	4.1	23.3	1.0	60.4	61.7	58.6	78.0
mPLUG-Owl3-7B									
Vanilla	11.6	6.6	5.4	8.3	1.4	50.8	48.3	43.3	55.0
ViPSy (Ours)	9.6	5.9	4.8	7.8	1.1	54.6	48.2	45.3	56.8
InternVL3.5-8B									
Vanilla	8.3	4.6	4.3	24.6	1.5	64.2	66.3	59.3	81.6
ViPSy (Ours)	7.3	4.2	3.9	17.3	1.2	65.4	67.9	60.0	81.4
Kimi-VL-A3B									
Vanilla	5.6	3.5	5.9	38.8	3.8	56.0	49.5	48.6	75.8
ViPSy (Ours)	5.0	3.1	4.1	29.4	1.9	57.7	52.2	50.0	76.4

F Algorithm

Algorithm 1 presents the ViPSy preference construction pipeline. For each image-prompt pair, ViPSy first generates multiple self-captions using the policy model and synthesizes semantic image variants with a text-to-image model. A judge model compares each variant with the original image to extract shared object-level evidence, and aggregates these pairwise cues into a consistent visual cue. Then, the policy model samples multiple responses conditioned on the original prompt, image, and visual cue. The judge selects the most visually grounded candidate as the preferred response and the least grounded candidate as the dispreferred response, forming a preference pair. The synthetic images and visual cues are used only for constructing preference data and are not required during inference.

G Additional results

We provide the full results discussed in Section 4. Specifically, Hal. AVG. denotes the average score over Object HalBench and AMBER, which measure hallucination in generated responses. Gen. AVG. denotes the average score over MMStar, MMVP, and CV-Bench, which are used to evaluate general vision-language capabilities in Section 4.

G.1 Policy model ablation

Table 6 reports the results of applying preference alignment to different policy models using policy-specific preference data constructed by ViPSy. The results show that ViPSy not only mitigates hallucination but also improves general vision-language capabilities. This indicates that ViPSy is not limited to a single policy model and can generalize across different VLMs.

G.2 Model component ablation

In Table 7, we analyze how each model component in ViPSy affects performance. We vary the image-to-text captioning model, the text-to-image synthesis model, and the rollout model used in ViPSy. The comparison highlights that self-captioning and self-rollouts are important for keeping the constructed preference data close to the policy distribution, while the choice of text-to-image model has a smaller effect.

G.3 Number of rollouts ablation

Table 8 reports the results for different numbers of cue-conditioned rollouts. Overall, increasing the number of rollouts generally improves performance across both hallucination and general benchmarks, as a larger candidate pool provides more diverse responses for preference selection. In particular,

Table 7: Results on hallucination and general benchmarks using LLaVA-1.5-7B. We vary the image-to-text captioning model (I→T), the text-to-image synthesis model (T→I), and the rollout model while keeping the remaining components fixed. “Self” denotes using the policy model itself.

ViPSy Configuration			Hallucination benchmarks					General benchmarks			
I→T	T→I	Rollout	Object HalBench		AMBER		Hal. Bench	MMStar	MMVP	CV-Bench	
			Resp.↓	Ment.↓	CHAIR↓	Hal.↓	Cog.↓	aAcc.↑	Acc.↑	Acc.↑	
<i>Vanilla (LLaVA-1.5-7B)</i>			51.3	25.9	7.9	36.8	4.3	46.8	33.4	23.3	61.9
Self	SD-3.5-L	Self	4.0	2.6	1.8	9.6	0.6	48.1	35.4	30.6	64.4
GPT-5 mini	SD-3.5-L	Self	6.6	4.4	1.9	12.0	0.7	47.2	33.8	29.3	64.6
Qwen3-VL-30B	SD-3.5-L	Self	4.6	3.5	2.2	12.4	0.8	47.9	34.4	28.0	64.0
Qwen2.5-VL-72B	SD-3.5-L	Self	4.0	2.2	2.1	12.1	0.9	47.7	34.8	29.3	63.1
Self	PixelDiT	Self	3.3	2.4	2.4	13.5	0.9	48.7	34.7	28.6	64.8
Self	Flux-1.0-dev	Self	4.6	3.1	2.3	11.1	0.7	48.7	34.6	29.3	63.6
Self	SD-3.5-M	Self	4.3	2.6	1.7	10.1	0.6	48.2	34.6	29.3	64.7
Self	SD-3.5-L	GPT-5 mini	30.6	15.1	5.3	24.3	2.9	47.7	33.0	28.0	62.2
Self	SD-3.5-L	Qwen3-VL-30B	29.6	16.6	5.1	25.6	3.1	47.9	33.1	30.6	62.5
Self	SD-3.5-L	Qwen2.5-VL-72B	21.6	10.4	3.8	18.5	1.8	47.7	33.7	28.6	63.1

Table 8: Results on hallucination and general benchmarks using LLaVA-1.5-7B. We compare preference construction with different numbers of cue-conditioned rollouts. For each rollout setting, we report the mean and standard deviation over five runs.

Number of Rollouts	Hallucination benchmarks					General benchmarks			
	Object HalBench [87]		AMBER [88]		Hal. Bench [22]	MMStar [89]	MMVP [90]	CV-Bench [91]	
	Resp.↓	Ment.↓	CHAIR↓	Hal.↓	Cog.↓	aAcc.↑	Acc.↑	Acc.↑	
Vanilla	51.3	25.9	7.9	36.8	4.3	46.8	33.4	23.3	61.9
8	3.67 ± 0.53	2.54 ± 0.26	1.92 ± 0.29	9.68 ± 1.52	0.64 ± 0.13	48.25 ± 0.67	35.39 ± 0.67	30.53 ± 1.85	64.27 ± 0.37
2	4.73 ± 0.55	2.84 ± 0.40	2.82 ± 0.34	13.16 ± 1.66	0.78 ± 0.13	47.65 ± 0.61	34.00 ± 0.21	29.27 ± 1.21	63.06 ± 0.62
4	4.33 ± 0.91	2.86 ± 0.53	2.38 ± 0.19	11.90 ± 1.23	0.72 ± 0.13	47.55 ± 0.52	34.59 ± 0.25	29.47 ± 1.66	63.79 ± 0.32
16	3.33 ± 0.33	1.84 ± 0.10	2.08 ± 0.04	9.40 ± 0.40	0.64 ± 0.05	48.83 ± 0.20	35.41 ± 0.10	30.73 ± 0.60	64.02 ± 0.19

using more rollouts enables the judge to compare candidates with different grounding quality under the same image, prompt, and visual cue, resulting in more informative preference pairs for training. While 16 rollouts further improve several metrics, the gains over 8 rollouts are relatively marginal, and 8 rollouts even achieve better performance on CV-Bench. Considering the additional computational cost incurred by generating more rollouts, we choose 8 rollouts as a practical default.

G.4 Preference selection judge ablation

Table 9 provides the complete benchmark results under different preference selection judge models. Since the judge selects preferred and dispreferred responses from multiple candidates, this ablation examines whether ViPSy depends on a particular judge model. The results remain stable across judges, indicating that the preference selection process is robust to the choice of judge model.

G.5 Synthesis strategy ablation

Table 10 reports results for cue conditioning and visual variation strategies used for cue extraction. The no-cue setting still benefits from policy self-sampling, but it is less effective than cue-conditioned preference construction, indicating that grounded visual cues are important for guiding rollouts toward visually faithful responses. For visual variation, simple transformations such as translation, resizing, masking, and cropping improve performance but provide limited semantic diversity. Video-based variation uses an image-to-video model [98] to generate candidate frames from the input image. We then compute the cosine similarity between the visual features of the original image and each generated frame, and sample frames whose similarity is closest to 0.8. This selection encourages moderate visual variation while maintaining semantic consistency with the original image. However, despite this filtering, uncontrolled changes across generated frames can still make the extracted cues less reliable. In contrast, diffusion-based semantic synthesis produces richer semantic variations and achieves the strongest overall results, showing that semantically diverse visual variations help extract more consistent and reliable object-level cues.

Table 9: Results on hallucination and general benchmarks using LLaVA-1.5-7B. We compare preference construction by varying the preference selection judge in ViPSy.

Judge	Hallucination benchmarks						General benchmarks		
	Object HalBench [87]		AMBER [88]			Hal. Bench [22]	MMStar [89]	MMVP [90]	CV-Bench [91]
	Resp.↓	Ment.↓	CHAIR↓	Hal.↓	Cog.↓	aAcc.↑	Acc.↑	Acc.↑	Acc.↑
GPT-5 mini	3.3	2.2	1.9	9.6	0.5	48.1	34.5	27.3	64.7
Qwen3-VL-30B	3.3	2.2	2.0	9.8	0.7	47.7	35.0	28.0	64.4
Qwen2.5-VL-72B	4.0	2.6	1.8	9.6	0.6	48.1	35.4	30.6	64.4

Table 10: Results on hallucination and general benchmarks using LLaVA-1.5-7B. We compare preference construction without visual cues, simple image transformations (translation, resize, mask, and crop), video-based variation, and diffusion-based semantic synthesis.

Strategy	Hallucination benchmarks						General benchmarks		
	Object HalBench [87]		AMBER [88]			Hal. Bench [22]	MMStar [89]	MMVP [90]	CV-Bench [91]
	Resp.↓	Ment.↓	CHAIR↓	Hal.↓	Cog.↓	aAcc.↑	Acc.↑	Acc.↑	Acc.↑
Vanilla	51.3	25.9	7.9	36.8	4.3	46.8	33.4	23.3	61.9
w/o cue	7.6	3.9	3.3	19.7	1.2	47.1	34.3	28.6	64.6
Translation	5.3	4.6	2.3	12.5	0.8	48.6	34.3	30.6	64.5
Resize	4.3	3.2	2.4	13.4	0.8	47.2	35.0	26.6	65.8
Mask	5.0	3.7	2.4	12.5	0.5	47.2	34.9	28.0	64.7
Crop	5.0	3.9	2.3	11.8	0.8	47.6	34.6	28.0	64.7
Video	4.3	3.4	2.3	11.5	0.8	48.0	33.2	28.0	63.9
Diffusion	4.0	2.6	1.8	9.6	0.6	48.1	35.4	30.6	64.4

G.6 Variance of the ViPSy

In the main experiments, we follow prior work and use temperature 0 during inference, which removes randomness in generation and ensures a fair comparison with existing hallucination-mitigation methods. Since VLM outputs can vary when using a nonzero temperature, we further examine the inference-time variance of the model preference-aligned with ViPSy-constructed data. Specifically, we set the temperature to 0.7 and repeat inference five times. As shown in Table 11, which summarizes the mean and standard deviation across the five runs, the model preference-aligned with ViPSy-constructed data achieves lower mean hallucination scores than the vanilla model on Object HalBench and AMBER, while achieving higher mean scores on HallusionBench and general vision-language benchmarks. Overall, these results show that preference alignment with ViPSy-constructed data maintains its hallucination-mitigation effect while enhancing general vision-language capability under repeated inference with temperature 0.7.

H Qualitative results

We provide additional qualitative comparisons to illustrate how ViPSy constructs preference data and how the aligned model behaves after training. We also provide examples of our proposed self-captioned semantic synthesis pipeline, which visualizes how synthetic image variations are generated from policy-generated captions.

H.1 Preference data examples

Figure 6 shows additional examples of preference pairs constructed by ViPSy. Each example contains the image, the prompt, the extracted visual cue, and the selected preferred and dispreferred responses. The preferred responses describe objects and relations supported by the image and visual cue, whereas the dispreferred responses include information that is not present in the image. These examples show that cue-conditioned self-rollouts produce candidate responses with different degrees of visual grounding, enabling the judge to select informative preference pairs for preference alignment.

Table 11: Variance of ViPSy on LLaVA-1.5-7B. Results are computed over five inference runs with temperature 0.7 and reported as mean and standard deviation.

Method	Hallucination benchmarks						General benchmarks		
	Object HalBench [87]		AMBER [88]			Hal. Bench [22]	MMStar [89]	MMVP [90]	CV-Bench [91]
	Resp.↓	Ment.↓	CHAIR↓	Hal.↓	Cog.↓	aAcc.↑	Acc.↑	Acc.↑	Acc.↑
Vanilla	53.0 ± 1.9	27.7 ± 1.1	9.3 ± 0.8	41.7 ± 3.0	4.3 ± 0.2	46.4 ± 0.3	33.0 ± 0.8	27.0 ± 2.4	57.8 ± 2.4
ViPSy (Ours)	4.1 ± 0.4	2.8 ± 0.5	2.0 ± 0.3	10.2 ± 1.3	0.6 ± 0.1	47.8 ± 0.8	34.4 ± 0.9	29.8 ± 1.1	64.6 ± 1.4

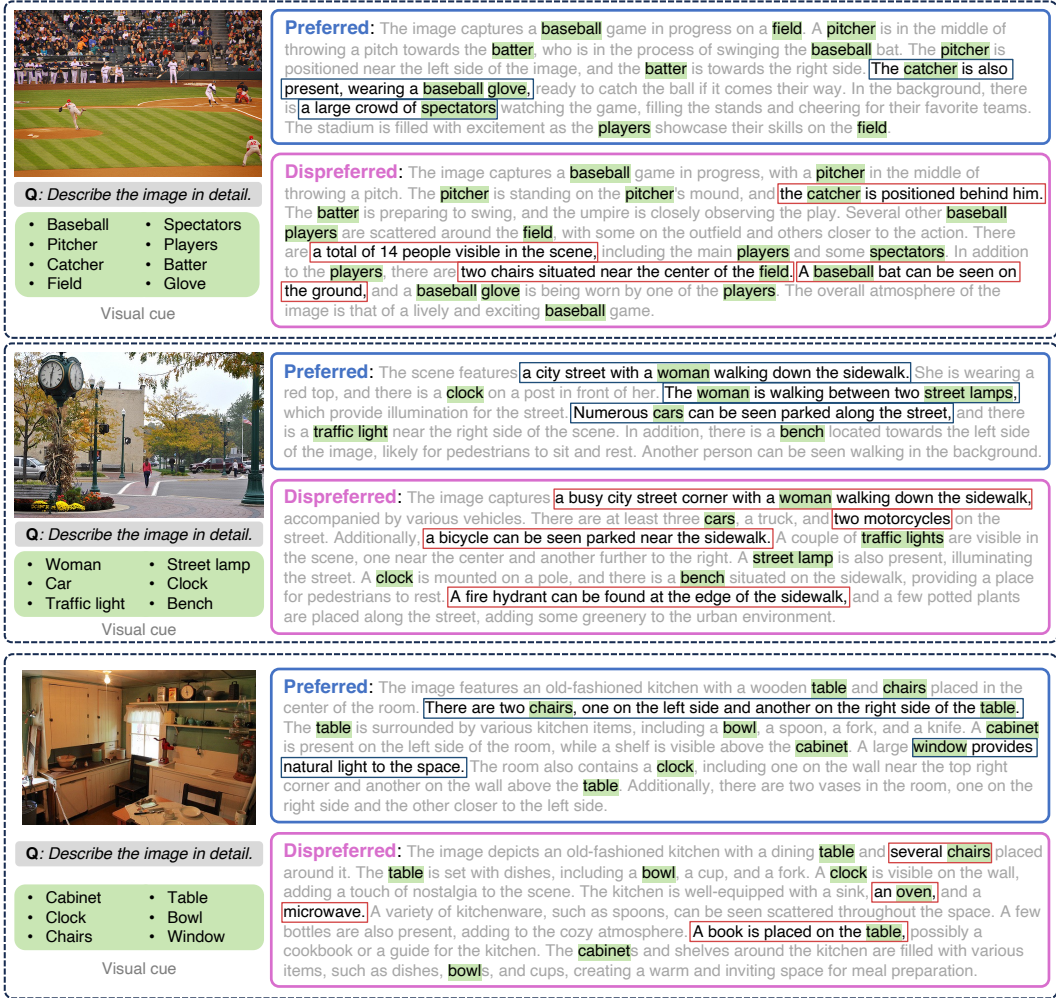


Figure 6: Qualitative examples of cue-conditioned preference pairs. Given the same image, prompt, and visual cue, preferred responses remain image-grounded, while dispreferred ones hallucinate.

H.2 Image description examples

Figure 7 compares image descriptions from the vanilla model and the model preference-aligned using preference pairs constructed by ViPSy. The vanilla model often includes hallucinated details that are not supported by the image. In contrast, the model trained with ViPSy produces descriptions that are better grounded in the image. This supports the effectiveness of the proposed preference construction in reducing hallucination.

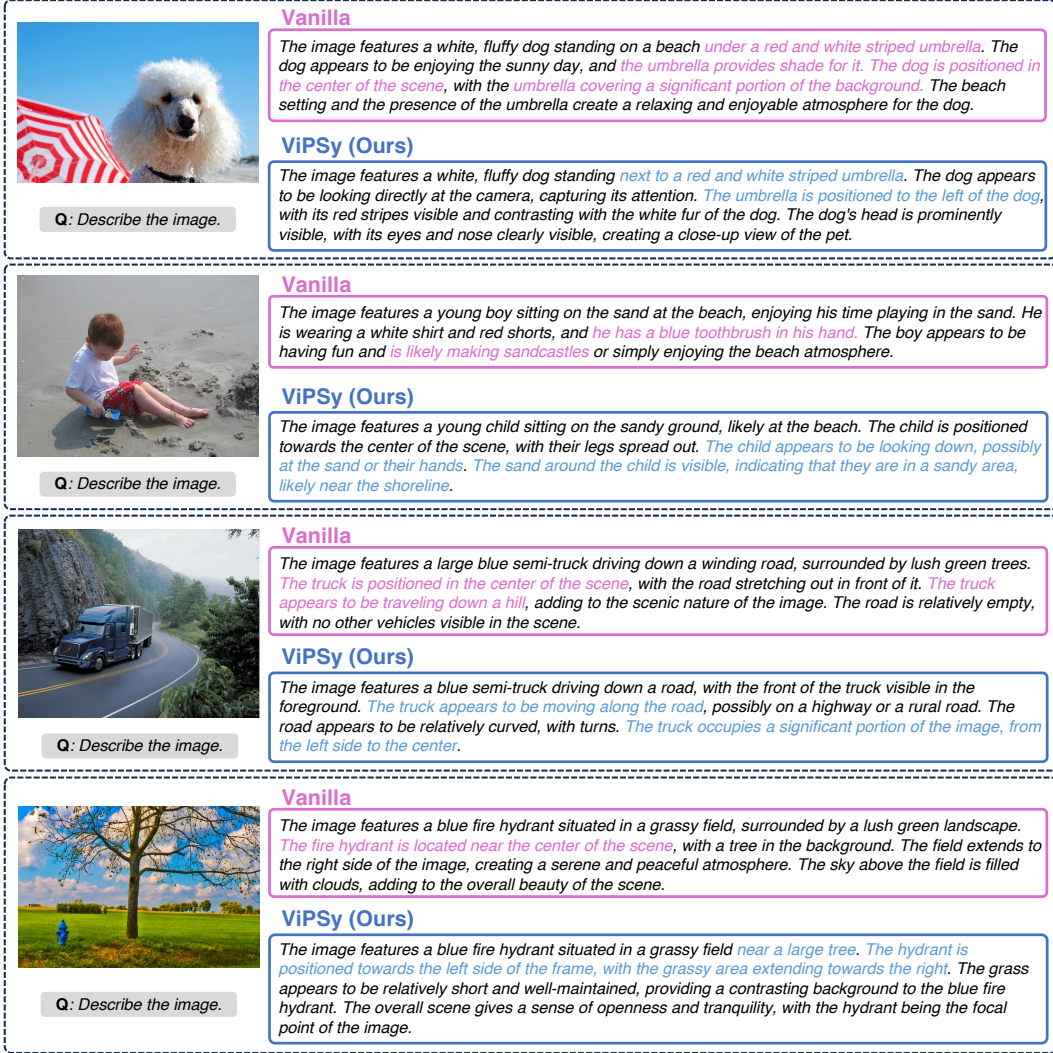


Figure 7: Qualitative comparison between the vanilla model and the model preference-aligned using preference pairs constructed by ViPSy. After preference alignment, the aligned model produces image-grounded descriptions, whereas the vanilla model describes content that is not present in the image. Highlights indicate image-inconsistent descriptions for the vanilla model and grounded descriptions for the preference-aligned model.

H.3 Self-captioned semantic synthesis examples

Figures 8 and 9 illustrate examples of self-captioned semantic synthesis. For each source image, the policy first generates a self-caption, which is then used as a prompt for text-to-image synthesis. Although the synthetic images vary in appearance, recurring objects and scene elements across the original and synthetic images provide reliable evidence for constructing the visual cue. These examples show how semantic diversity from synthesis helps ViPSy extract image-grounded object-level cues.

I Prompts

We list prompts used in ViPSy for preference construction. For self-captioning, we use the prompt “Describe the image in detail.” The pairwise comparison prompt $x_{\text{comp.}}$ in Figure 10, the aggregation prompt $x_{\text{agg.}}$ in Figure 11, the cue-conditioned captioning prompt $x_{\text{cue-cap.}}$ in Figure 12, and the visual grounding prompt $x_{\text{vis.}}$ in Figure 13 are used for cue extraction and preference construction.

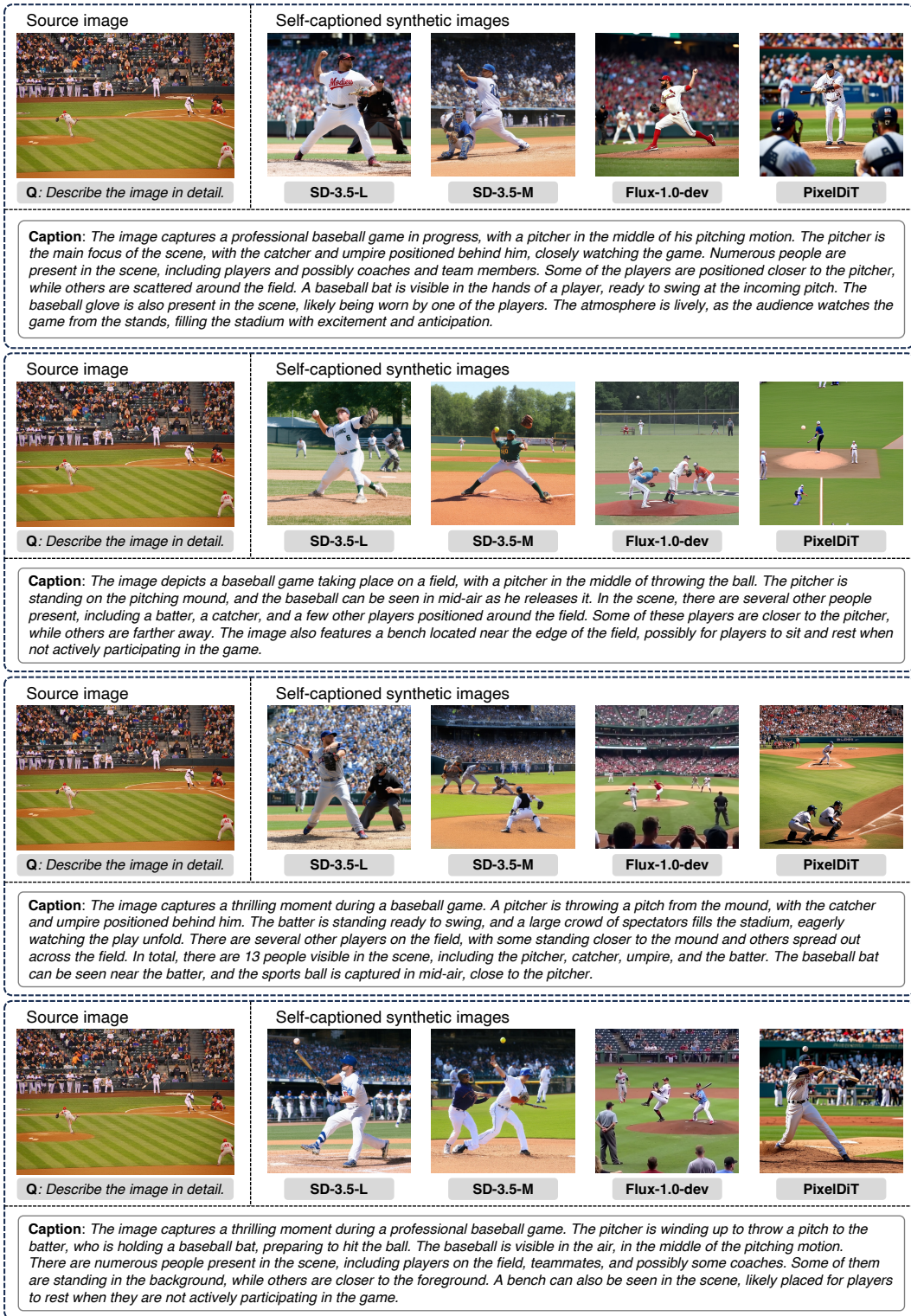


Figure 8: Examples of self-captioned semantic synthesis. The source image is first captioned by the policy model, and the caption is used to generate semantically aligned synthetic images using the text-to-image models SD-3.5-L, SD-3.5-M, Flux-1.0-dev, and PixelDiT.

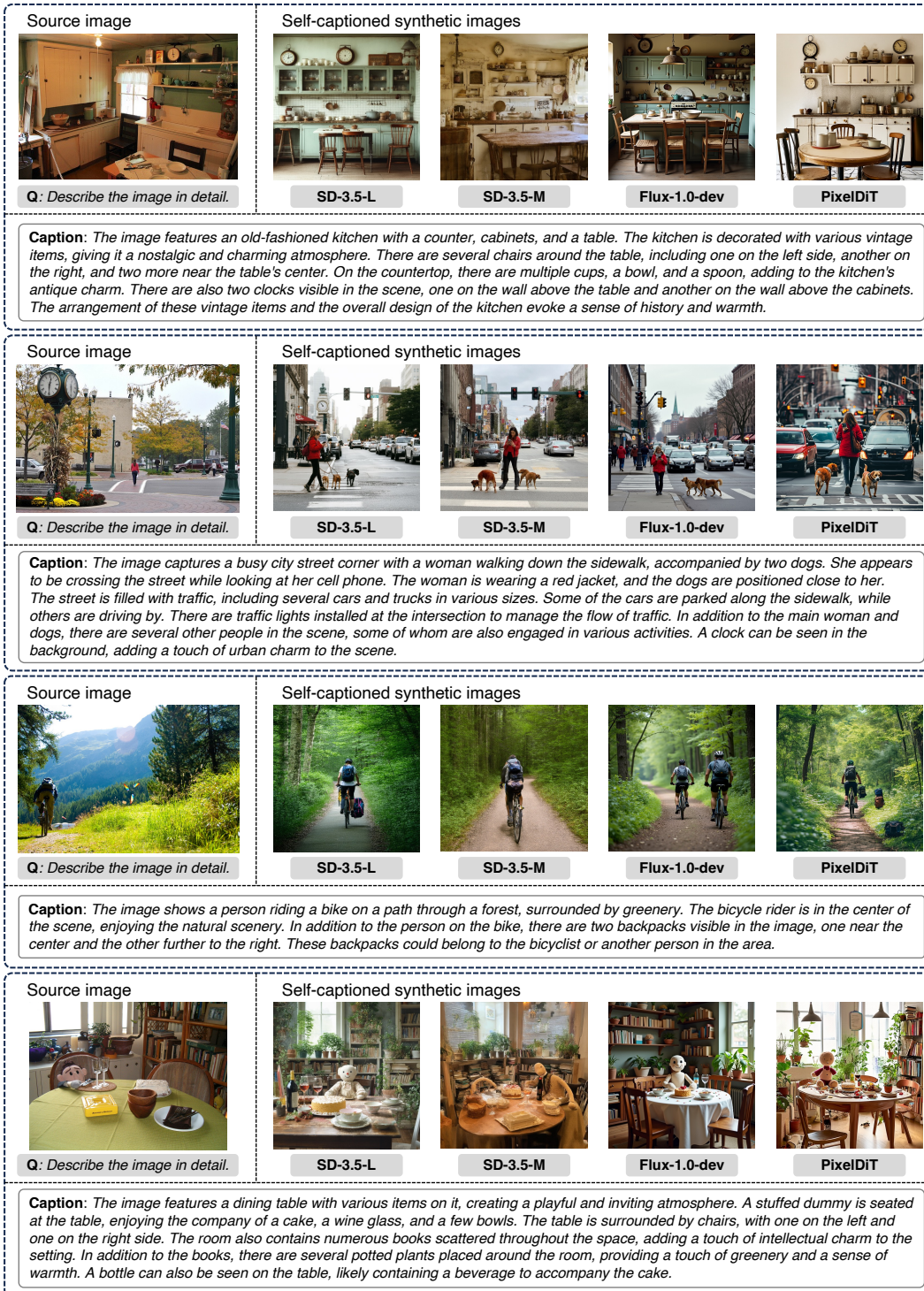


Figure 9: Examples of self-captioned semantic synthesis. The source image is first captioned by the policy model, and the caption is used to generate semantically aligned synthetic images using the text-to-image models SD-3.5-L, SD-3.5-M, Flux-1.0-dev, and PixelDiT.

Compare two images. The first image is the reference image. The second image is the comparison image. Keep only clearly shared facts. Do not include differences, unique details or extra keys. Keep phrases short, factual and reusable. If uncertain, omit it.

{*an image pair*}

Figure 10: Pairwise comparison prompt.

You are given pairwise comparison results between one reference image and multiple comparison images. Each pairwise result contains shared facts. Merge similar phrases, remove near-duplicates, and produce one consolidated result.

Rules:

- chosen should contain the merged shared content from the pairwise chosen results.
- Keep only content that is supported as shared visual content across the pairwise chosen results.
- Merge synonymous or near-duplicate phrases into one natural phrase.
- Prefer short, reusable, neutral wording.
- Do not invent new facts that are not supported by the pairwise results.
- Do not mention pair indices, or phrases like 'in comparison image'.
- If a fact is uncertain, omit it.

{*pairwise visual cues*}

Figure 11: Aggregation prompt.

Describe the image in detail.

Please use the following object information as extra context: {*visual cues*}

Figure 12: Cue-conditioned captioning prompt.

You are evaluating candidate responses for DPO data construction.

You are given:

1. The original image
2. Multiple candidate responses generated from repeated inference runs on the same original image

Important:

- Use the original image as the main visual evidence.

Your task:

Select:

- the single best candidate response
- the single worst candidate response

Selection criteria:

- The best candidate should be the most visually grounded to the original image and should avoid unsupported details.
- The worst candidate should be the least grounded, adding unsupported objects, people, actions, attributes, or scene details.
- Prefer a worst candidate that is plausible but likely unsupported rather than one that is merely short or generic.

{*candidates*}

Figure 13: Visual grounding prompt.